














# EDS1 complexes are not required for PRR responses and execute TNL-ETI from the nucleus in *Nicotiana benthamiana*

Josua Zönnchen<sup>1\*</sup> , Johannes Gantner<sup>1\*</sup> , Dmitry Lapin<sup>2,3\*</sup> , Karen Barthel<sup>1</sup> ,  
 Lennart Eschen-Lippold<sup>4,5</sup> , Jessica L. Erickson<sup>5</sup> , Sergio Landeo Villanueva<sup>6</sup> , Stefan Zantop<sup>1</sup> ,  
 Carola Kretschmer<sup>1</sup> , Matthieu H. A. J. Joosten<sup>6</sup> , Jane E. Parker<sup>2,7</sup> , Raphael Guerois<sup>8</sup>  and  
 Johannes Stüttmann<sup>1,9</sup> 

<sup>1</sup>Department of Plant Genetics, Institute for Biology, Martin Luther University Halle-Wittenberg, D-06120 Halle, Germany; <sup>2</sup>Department of Plant–Microbe Interactions, Max-Planck Institute for Plant Breeding Research, D-50829 Cologne, Germany; <sup>3</sup>Department of Biology, Plant–Microbe Interactions, Utrecht University, 3584 CH Utrecht, the Netherlands; <sup>4</sup>Department of Crop Physiology, Institute of Agricultural and Nutritional Sciences, Martin Luther University Halle-Wittenberg, D-06120, Halle Germany; <sup>5</sup>Department of Biochemistry of Plant Interactions, Leibniz Institute of Plant Biochemistry, D-06120 Halle, Germany; <sup>6</sup>Laboratory of Phytopathology, Wageningen University and Research, 6708 PB Wageningen, the Netherlands; <sup>7</sup>Cologne–Düsseldorf Cluster of Excellence in Plant Sciences (CEPLAS), D-40225 Düsseldorf, Germany; <sup>8</sup>Institute for Integrative Biology of the Cell (I2BC), IBITECS, CEA, CNRS, Université Paris-Saclay, F-91198 Gif-sur-Yvette, France; <sup>9</sup>Institute for Biosafety in Plant Biotechnology, Federal Research Centre for Cultivated Plants, Julius Kühn-Institute (JKI), 06484 Quedlinburg, Germany

## Summary

Author for correspondence:

Johannes Stüttmann

Email: johannes.stuttmann@julius-kuehn.de

Received: 5 January 2022

Accepted: 2 September 2022

*New Phytologist* (2022) **236**: 2249–2264

doi: 10.1111/nph.18511

**Key words:** *Arabidopsis thaliana*, BAK1, EDS1, innate immunity, *Nicotiana benthamiana*, NLR, pattern recognition receptors (PRRs), TNL receptor.

- Heterodimeric complexes incorporating the lipase-like proteins EDS1 with PAD4 or SAG101 are central hubs in plant innate immunity. EDS1 functions encompass signal relay from TIR domain-containing intracellular NLR-type immune receptors (TNLs) towards RPW8-type helper NLRs (RNLs) and, in *Arabidopsis thaliana*, bolstering of signaling and resistance mediated by cell-surface pattern recognition receptors (PRRs). Increasing evidence points to the activation of EDS1 complexes by small molecule binding.
- We used CRISPR/Cas-generated mutant lines and agroinfiltration-based complementation assays to interrogate functions of EDS1 complexes in *Nicotiana benthamiana*.
- We did not detect impaired PRR signaling in *N. benthamiana* lines deficient in EDS1 complexes or RNLs. Intriguingly, in assays monitoring functions of *S/EDS1-NbEDS1* complexes in *N. benthamiana*, mutations within the *S/EDS1* catalytic triad could abolish or enhance TNL immunity. Furthermore, nuclear EDS1 accumulation was sufficient for *N. benthamiana* TNL (Roq1) immunity.
- Reinforcing PRR signaling in *Arabidopsis* might be a derived function of the TNL/EDS1 immune sector. Although Solanaceae EDS1 functionally depends on catalytic triad residues in some contexts, our data do not support binding of a TNL-derived small molecule in the triad environment. Whether and how nuclear EDS1 activity connects to membrane pore-forming RNLs remains unknown.

## Introduction

Genetically encoded cell surface-resident and intracellular immune receptors serve as detection devices in plant and animal innate immunity. In plants, which lack an adaptive immune system, immune receptor repertoires have expanded and diversified between different species or even accessions (Barragan & Weigel, 2021). At the cell surface, pattern recognition receptors (PRRs) detect microbe-associated molecular patterns (MAMPs) to induce pattern-triggered immunity (PTI). Inside the cell, receptors of the nucleotide-binding/leucine rich repeat (NLR) class detect effector proteins (virulence factors secreted into the

host cell cytoplasm by pathogenic microbes) to induce effector-triggered immunity (ETI).

Pattern recognition receptors are receptor-like kinases (RLKs) or receptor-like proteins (RLPs) with diverse ectodomains (reviewed in Saijo *et al.*, 2018). RLKs and RLPs associate, either constitutively or in a stimulus-dependent manner, with co-receptors, such as the RLKs BAK1/SERK3 (Brassinosteroid-insensitive 1 (BRI1) Associated Kinase1/Somatic Embryogenesis Receptor Kinase 3) or SOBIR1 (Suppressor Of BIR1,1; Chinchilla *et al.*, 2007; Heese *et al.*, 2007; Liebrand *et al.*, 2013). PRR-ligand binding induces a suite of downstream signaling events and physiological responses, including activation of mitogen-activated protein kinases (MAPKs), Ca<sup>2+</sup>-influx,

\*These authors contributed equally to this work.

production of reactive oxygen species (ROS) and ethylene, and induction of defense genes (Saijo *et al.*, 2018). Some PRRs detect pathogen isolate-specific ligands, such as apoplastic effectors of the fungal pathogens *Verticillium dahliae* and *Cladosporium fulvum*, to induce strong resistance responses accompanied by programmed cell death (Thomma *et al.*, 2011). However, most characterized MAMPs are relatively conserved molecules characteristic for a class or group of organisms, such as fungal chitin or peptides derived from bacterial flagellin (Saijo *et al.*, 2018). Activation of the respective PRRs (e.g. FLS2; Flagellin-Sensitive 2) is not normally accompanied by cell death. Accordingly, PTI is generally considered a low-level resistance response sufficient to combat nonadapted pathogens.

Host-adapted pathogens that overcome PTI confront the ETI defense layer. A rapid and strong ETI response, often accompanied by programmed cell death at infection sites (the hypersensitive response, HR), is induced in the presence of an effector and a matching NLR-type immune receptor. The canonical NLR architecture consists of a C-terminal leucine-rich repeat (LRR), a central nucleotide-binding/oligomerization and an N-terminal signaling domain (Bentham *et al.*, 2017). Plant NLRs are subdivided into three major classes based on their N-terminal domains: TNLs carrying a Toll-interleukin 1 receptor (TIR) domain, CNLs carrying a coiled coil (CC) domain, and RNLs carrying a CC<sub>R</sub> or HeLo domain, a subtype of the CC domain also found in the non-NLR immunity regulators RPW8 and MLKL (Resistance to Powdery Mildew 8 and Mixed Lineage Kinase-Like; Xiao *et al.*, 2005; Collier *et al.*, 2011; Lapin *et al.*, 2020; Mahdi *et al.*, 2020). Most characterized CNLs and TNLs function as sensor NLRs (sNLRs) in pathogen effector detection. sNLR repertoires are diverse and can range from a few to several hundred *NLR* genes (Baggs *et al.*, 2020). By contrast, RNLs are more conserved and operate in basal resistance against virulent pathogens and as helper NLRs (hNLRs) downstream of TNLs and some CNLs (Bonardi *et al.*, 2011; Castel *et al.*, 2018; Wu *et al.*, 2018; Lapin *et al.*, 2019; Saile *et al.*, 2020; Sun *et al.*, 2021). Two subgroups of RNLs, ADR1 (Activated Disease Resistance 1) and NRG1 (N-Required Gene 1) RNLs, were detected in the genomes of nearly all flowering plants (Collier *et al.*, 2011).

Although ADR1s are present in seed plant genomes, NRG1s are restricted to eudicots with expanded TNL panels (Collier *et al.*, 2011; Lapin *et al.*, 2020; Liu *et al.*, 2021). Recent reports suggest that sensor CNLs and RNL-type hNLRs form oligomers (resistosomes) upon activation, which can insert into membranes and function as cation-permeable channels (Wang *et al.*, 2019; Bi *et al.*, 2021; Jacob *et al.*, 2021). Although it remains unclear whether resistosome formation by *Arabidopsis thaliana* (Arabidopsis) CNL ZAR1 (HopZ-Activated Resistance 1) is prototypical for CNLs and RNLs, it is possible that Ca<sup>2+</sup> influx represents a common output in CNL and TNL-RNL immunity (Bernoux *et al.*, 2022; Parker *et al.*, 2022).

Traditionally, PTI and ETI were considered as independent immune sectors contributing to pathogen resistance and converging on transcriptional defenses (Tao *et al.*, 2003; Cui *et al.*, 2015). Recent reports suggest that ETI and PTI cross-potentiate

each other in pathogen resistance (Lu & Tsuda, 2021). PTI-deficient Arabidopsis lines failed to mount efficient ETI responses (Ngou *et al.*, 2021; Yuan *et al.*, 2021). Reciprocally, ETI components were required for PTI in Arabidopsis: lines deficient in a central regulator of TNL immunity, EDS1 (Enhanced Disease Susceptibility 1) or RNLs were unable to mount full TNL immunity and were impaired in early and late PTI responses (Pruitt *et al.*, 2021; Tian *et al.*, 2021). Likewise, in Solanaceae, at least some RLPs require NLRs of the NRC (NLR Required for Cell Death) superclade, and attenuation of PTI responses in EDS1-deficient plants was suggested (Hu *et al.*, 2005; Gabriels *et al.*, 2006, 2007; Fradin *et al.*, 2009; Kourelis *et al.*, 2021). However, molecular mechanisms underlying PTI-ETI connectivity remain unknown. For example, it is unclear whether EDS1 contributes directly to PTI signaling or whether PTI signaling is primed and reinforced by TNL/TIR protein signaling via EDS1 (Pruitt *et al.*, 2021; Tian *et al.*, 2021).

EDS1 is part of a small plant-specific protein family also containing PAD4 (Phytoalexin-Deficient 4) and SAG101 (Senescence Associated Gene 101; Lapin *et al.*, 2020). EDS1 family proteins are characterized by the fusion of an  $\alpha/\beta$ -hydrolase (class-3 lipase) domain with a C-terminal EP (EDS1-PAD4) all-helical domain which has no significant similarities to any known structure (Wagner *et al.*, 2013; Bhandari *et al.*, 2019). EDS1 forms mutually exclusive heterodimers with PAD4 or SAG101 (Wagner *et al.*, 2013). In Arabidopsis, the EDS1-PAD4 complex together with ADR1 proteins is required for TNL-mediated pathogen resistance and reinforces signaling by surface receptors (Pruitt *et al.*, 2021; Tian *et al.*, 2021). By contrast, EDS1-SAG101 dimers in association with NRG1s promote TNL-triggered defense and regulate host cell death (Lapin *et al.*, 2019; Dongus & Parker, 2021; Sun *et al.*, 2021; Wu *et al.*, 2021).

In our current understanding, EDS1 complexes operate downstream of TNL receptors but upstream of RNLs, because autoactive RNL fragments, but not TNL activation or autoactive TNLs and isolated TIR domains, can induce cell death and resistance signaling in *eds1* mutant plants (Qi *et al.*, 2018; Horsefield *et al.*, 2019; Wan *et al.*, 2019; Jacob *et al.*, 2021). Hence, EDS1 complexes probably relay a signal from activated TNLs to RNLs. Upon activation, the TNLs RPP1 (Recognition Of *Peronospora Parasitica* 1) and Roq1 (Recognition Of XopQ 1) tetramerize into holoenzymes with NADase activity (Ma *et al.*, 2020; Martin *et al.*, 2020). Plant TIR-only proteins and/or isolated TNL-TIR domains can also function as NADase or 2',3'-cAMP/cGMP synthetase enzymes (Horsefield *et al.*, 2019; Wan *et al.*, 2019; Huang *et al.*, 2022; Jia *et al.*, 2022; Yu *et al.*, 2022), suggesting that signal relay is mediated by TIR-domain-generated small molecules. One candidate binding site is represented by lipase-like domain pockets with a characteristic serine-aspartate-histidine catalytic triad conserved in the N-terminal domains of EDS1 and PAD4 (but not SAG101) orthologs, which could bind and/or process a TNL-generated small molecule (Wagner *et al.*, 2013; Voss *et al.*, 2019).

We established *Nicotiana benthamiana* (*Nb*) as a genetic system for analysis of EDS1-family functions in TNL immunity (Adlung *et al.*, 2016; Ordon *et al.*, 2017; Gantner *et al.*, 2019).

Our analyses revealed that, in contrast to *Arabidopsis*, an EDS1-SAG101b complex (most Solanaceae genomes encode two SAG101 isoforms) is necessary and sufficient for all tested TNL-mediated immune responses in *Nb*; immune functions of *Nb*PAD4 were not detected (Gantner *et al.*, 2019). A TNL immune response also was largely abolished in NRG1-deficient *Nb* plants (Qi *et al.*, 2018), thus supporting a major role of the EDS1-SAG101-NRG1 module in regulating both pathogen resistance and cell death during TNL ETI in *Nb*.

In this study, we investigated EDS1 dimer functions and the subcellular compartments in which EDS1 complexes are localized during *Nb* PTI and ETI responses. In PTI assays, we fail to detect a role of EDS1-RNL modules in *Nb* PTI signaling, suggesting that PTI-ETI connectivity may be wired differently in *Nb* and *Arabidopsis*. In TNL-ETI assays monitoring the activity of heterologous *Nb*SAG101b-S $\Delta$ EDS1 (*Sl*-*Solanum lycopersicum*; tomato) complexes, exchanges within residues of the S $\Delta$ EDS1 catalytic triad enhance or abolish immune functions. However, co-expression of *SS*SAG101b restores immune capacities of functionally impaired S $\Delta$ EDS1 variants. Taken together with a careful in-depth analysis, our data disqualify the EDS1 triad environment as a small molecule binding site during TNL immunity. Further, our data suggest that mainly nuclear EDS1 complexes mediate immune signaling during an *Nb* ETI response. This puts into question the compartment in which RNLs, that are proposed to form plasma membrane pores, are activated and signal in Solanaceae TNL immunity.

## Materials and Methods

### Plant material and growth conditions

*Nicotiana benthamiana* (*Nb*) lines used were *Nb eds1a-1* (Ordon *et al.*, 2017), *pad4-1 sag101a-1 sag101b-1* (Gantner *et al.*, 2019), *nrg1-4* (Ordon *et al.*, 2021) and *eds1 pad4 sag101a sag101b* (*eps*; Lapin *et al.*, 2019). The *Nb bak1* mutant line was generated by CRISPR/Cas using previously described constructs (Stuttman *et al.*, 2021), and additional details are provided in Fig. S1 and Table S1. The *Nb adr1 nrg1* double mutant line is described in more detail elsewhere (Prautsch *et al.*, 2021). *Nb* plants were cultivated in a glasshouse with a 16 h : 8 h, light : dark photoperiod (sunlight and/or IP65 lamps (Philips) equipped with Agro 400 W bulbs (SON-T); 130–150  $\mu\text{E m}^{-2} \text{s}^{-1}$ ; switchpoint; 100  $\mu\text{E m}^{-2} \text{s}^{-1}$ ), 60% relative humidity (RH) at 24°C : 20°C, day : night. *Arabidopsis thaliana* (*Arabidopsis*) accession Columbia-0 was used. Plants were cultivated under short-day conditions (8 h : 16 h, light : dark photoperiod, 23°C : 21°C, day : night, 60% RH) or in a glasshouse under long-day conditions (16 h : 8 h, light : dark photoperiod) for seed set. An *eds1-12 pad4-1 sag101-3* triple mutant line was generated by crossing the *eds1-12* line (Ordon *et al.*, 2017) with a *pad4-1 sag101-3* double mutant line (Cui *et al.*, 2018).

### Molecular cloning and plant transformation

Gateway cloning and Golden Gate assembly were used to generate plant expression constructs using the Modular Cloning Plant

Toolbox, Plant Parts I and II collections (Engler *et al.*, 2014; Gantner *et al.*, 2018). See Tables S2 and S3 for plasmids and oligonucleotides used in this study, respectively. *Escherichia coli* Top10 and *ccdB* survival II and *Agrobacterium tumefaciens* strain GV3101 pMP90 were used. *Arabidopsis* plants were transformed by floral dipping (Logemann *et al.*, 2006). *Nb* transformation is described in an online resource (doi: 10.17504/protocols.io.sbacaie).

### Transient expression, infection and ion leakage assays

Transient protein expression in *Nb* (agroinfiltration) was conducted as described previously (Gantner *et al.*, 2019) at an OD<sub>600</sub> = 0.4 per strain, if not indicated otherwise. To measure ion leakage, leaf discs were harvested using a biopsy punch (5-mm) into 24-well plates. Leaf discs were washed 2 h, and conductivity was measured 24 h later (LAQUAtwin COND; Horiba Scientific, Kyoto, Japan). *Xanthomonas campestris* pv *vesicatoria* strain 85–10 (Thieme *et al.*, 2005) was used for mixed co-infiltrations and resistance assays, as described previously (Lapin *et al.*, 2019). *Pseudomonas syringae* pv *tomato* infection assays were conducted as described previously (Lapin *et al.*, 2019). Infections with *Hyaloperonospora arabidopsidis* (*Hpa*) and Trypan Blue staining were conducted as described previously (Stuttman *et al.*, 2011) using T<sub>1</sub> transgenic seeds selected by fluorescence (FAST; Shimada *et al.*, 2010). Red light imaging of cell death (Landeo Villanueva *et al.*, 2021) was conducted using a Fusion FX system (Vilber Lourmat Sté, Collégien, France). Intensity of cell death reactions was measured using IMAGEJ, and data were normalized to a 0–1 range.

### Immunodetection, protein co-purification and live cell imaging

Proteins were extracted by direct grinding of tissues in Laemmli buffer, denaturation, and clearing by centrifugation. Extracts were resolved on 8–12% SDS-PAGE gels, and transferred to nitrocellulose membranes for immunodetection. Membranes were stained with Ponceau or Amido black to control loading as described (Goldman *et al.*, 2016). Strep-Tactin-AP conjugate was used for detection of Strep-tagged proteins. Primary antibodies used were  $\alpha$ -GFP (mouse) and  $\alpha$ -hemagglutinin (rat; both from Roche) (GFP, green fluorescent protein). Horseradish peroxidase-coupled or alkaline phosphatase-coupled secondary antibodies were used. A Zeiss LSM780 confocal laser scanning microscope was used for live cell imaging. All images are single planes. DAPI staining was used to mark nuclei.

### PTI assays: ROS measurements

Production of ROS (hydrogen peroxide, H<sub>2</sub>O<sub>2</sub>) was measured in a 96-well plate format using leaf discs of 4-week-old *Nb* plants as described previously (Gomez-Gomez *et al.*, 1999). Briefly, 5-mm leaf discs were floated on H<sub>2</sub>O in microplates, incubated in the dark for 24 h, washed, and elicited with 2 nM flg22 or 100 nM Avr4. flg22-induced ROS burst was measured for 1 h

with a TriStar2 S LB942 luminescence plate reader (Berthold Technologies GmbH, Bad Wildbad, Germany). For measurements of Avr4-induced ROS production, leaf discs were sampled 2 d after infiltration of *Agrobacteria* for expression of Cf-4 (OD<sub>600</sub> = 0.1). Luminescence was measured over a period of 5 h on a CLARIOstar plate reader.

### Protein structural modeling

Models for the *A*EDS1-*A*SAG101, *A*EDS1-*A*SAG101-*A*NRG1 and *S*EDS1-*S*SAG101b complexes were generated running the ALPHAFOLD2 algorithm (Jumper *et al.*, 2021) via the ColabFold interface (Mirdita *et al.*, 2022). Models are available in ModelArchive ([www.modelarchive.org](http://www.modelarchive.org)) with identifiers ma-k5om5 (*A*EDS1-*A*SAG101), ma-ewx53 (*A*EDS1-*A*SAG101-*A*NRG1) and ma-cf7k5 (*S*EDS1-*S*SAG101). See Methods S1 for details.

## Results

### EDS1 complexes are dispensable for signaling by tested cell surface receptors in *N. benthamiana*

The EDS1-PAD4-ADR1 module fulfills a major immune function in Arabidopsis TNL-mediated pathogen resistance and contributes to PRR signaling (Dongus & Parker, 2021). By contrast, *Nb pad4* mutant plants were not impaired in TNL ETI assays (Gantner *et al.*, 2019; Lapin *et al.*, 2019). We therefore investigated whether the EDS1-PAD4 module or EDS1 complexes, together with RNLs, contribute to PRR signaling in Solanaceae, as suggested previously for *EDS1* (Hu *et al.*, 2005; Gabriels *et al.*, 2007).

We first generated an *Nb bak1/serk3* mutant line (referred to as *Nb bak1*) as a negative control for PRR signaling. In the *Nb bak1* line, two LRR-RLK-coding genes previously silenced by Heese *et al.* (2007) were disrupted by genome editing (Fig. S1; Table S1). *Nb bak1* mutant plants developed cell death similar to wild-type (WT) upon expression of several different effectors or an autoactive TIR fragment, suggesting that cell death pathways triggered intracellularly are not impaired (Fig. S2).

Alongside WT and *Nb bak1* plants, we tested induction of host cell death after activation of the tomato LRR-RLPs Cf-4 and Cf-9 (*Cladosporium fulvum*-4/9) in *Nb* mutant lines deficient in EDS1 complexes (*eds1* or *pad4 sag101a sag101b* (*ps*) triple mutant) or the RNL NRG1 (*nrg1*). Cf4 and Cf9 can be activated by transient co-expression of their respective *C. fulvum* ligands, Avr4 and Avr9 (Avirulence 4/9) in *Nb* (Van der Hoorn *et al.*, 2000). We observed reduced cell death on *Nb bak1* but not mutant lines deficient in EDS1 complexes or the RNL NRG1 (Figs 1a, S3a). We quantified cell death by ion leakage assays (Figs 1b, S3b). *Nb bak1* but none of the EDS1 complex- or RNL-deficient lines displayed lower ion leakage in the Cf4/Avr4-induced response (Fig. 1b). Cf9/Avr9-induced cell death is generally weaker (Van der Hoorn *et al.*, 2000) and we did not detect significant differences in ion leakage between lines (Fig. S3b). Furthermore, we

measured the Avr4-induced ROS burst in different *Nb* lines transiently expressing Cf-4 or GUS ( $\beta$ -glucuronidase; Fig. 1c). We included a mutant lacking all EDS1 proteins (*eps*s quadruple mutant; Lapin *et al.*, 2019) in these assays. Expression of Cf4, but not GUS, led to ROS burst induction upon elicitation with Avr4 (comparison wt-Cf-4 vs wt-GUS). The Avr4-induced ROS burst was reduced in *bak1*, but not in plants lacking EDS1 complexes (Fig. 1c).

We next tested PTI responses initiated by LRR-RLK *Nb*FLS2 in *Nb* mutant lines deficient in EDS1 complexes or RNLs, including an *Nb nrg1 adr1* double mutant (Fig. 1d; Prautsch *et al.*, 2021). A reduced ROS burst in *bak1* plants was not detected when using saturating flg22 concentrations (50 nM; Fig. S4a), although this was reported previously upon silencing of *BAK1-like* genes in *Nb* (Heese *et al.*, 2007). From dilution series, we selected 2 nM flg22 as suitable to induce a ROS burst under nonsaturating conditions (Fig. S4b,c). In corresponding assays of the mutant lines, flg22-elicited ROS production was significantly reduced in *Nb bak1*, but not in any other mutant (Fig. 1d).

In summary, the data show that neither EDS1 dimers nor RNLs are essential for the tested cell surface receptor-triggered immune responses in *Nb*. We concluded that recruitment of these components for PRR signaling probably does not represent a conserved function of EDS1, TNLs or RNLs between Arabidopsis and *Nb*.

### Exchanges within the catalytic triad can modulate Roq1 TNL immunity in *N. benthamiana* when *S*EDS1 functions in complex with *Nb*SAG101b

The EDS1-SAG101b complex mediates all known TNL immune functions in *Nb* and the C-terminal EP domains of both proteins are essential for TNL signaling (Gantner *et al.*, 2019; Lapin *et al.*, 2019). Here, we interrogated functions of the *S*EDS1 N-terminal lipase-like domain.

In the functional *S*EDS1-*S*SAG101b complex, *S*EDS1 but not *S*SAG101b, contains a conserved S–D–H catalytic triad (Fig. 2a; Wagner *et al.*, 2013; Gantner *et al.*, 2019). The critical serine residue (S125 in *S*EDS1) is embedded in a GX SXG motif forming the so-called nucleophile elbow (Fig. 2a; Rauwerdink & Kazlauskas, 2015). Previous analyses of *A*EDS1 revealed high spatial conservation with active lipases, but TNL-ETI did not require an intact triad (Wagner *et al.*, 2013). In models predicted by ALPHAFOLD2 (AF2), the N-terminal domains and catalytic triads of *A*EDS1 and *S*EDS1 have highly similar structures and spatial arrangements (Fig. S5a,b). An overlay of the *A*EDS1-*A*SAG101 AF2 model with the previously determined crystal structure shows quasi-identical structures in the N-terminal domains (Fig. S5c), suggesting that AF2 models of EDS1 complexes are reliable.

In *Nb*, TNL immunity and cell death can be induced by *Agrobacterium*-mediated transient expression of the *Xanthomonas campestris* pv *vesicatoria* (*Xcv*) effector XopQ (*Xanthomonas* Outer Protein Q), recognized by TNL Roq1 (Schultink *et al.*, 2017). In XopQ cell death assays, mutant lines deficient in *EDS1* family genes were transiently complemented by co-expression of

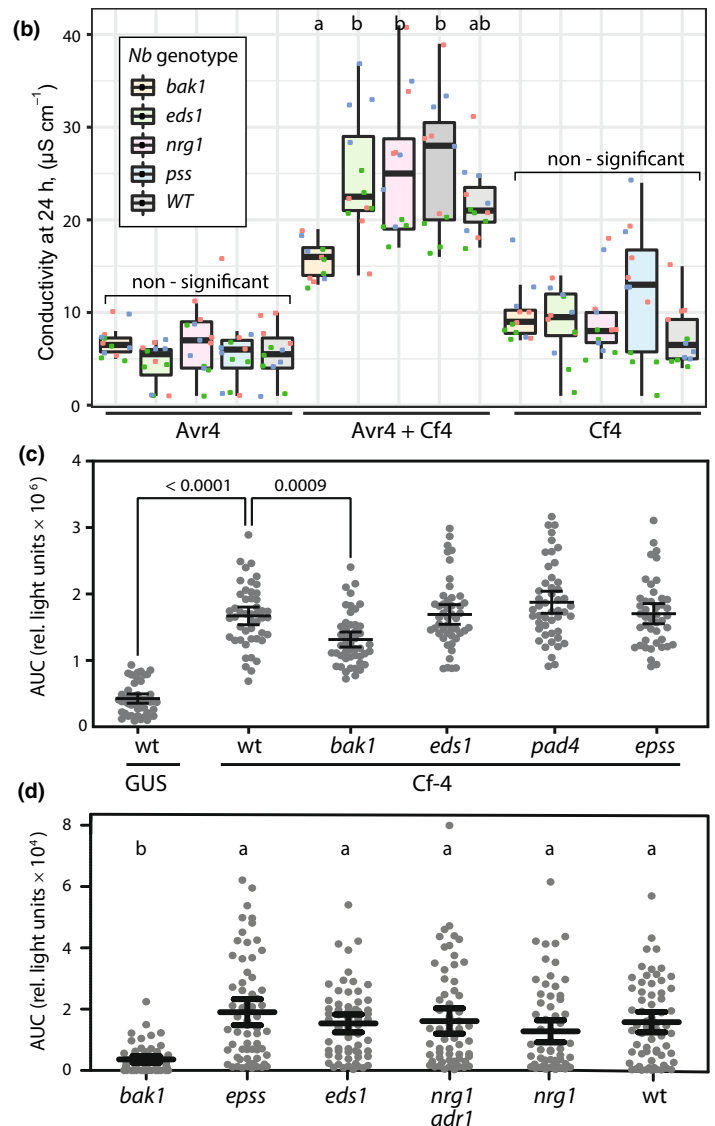
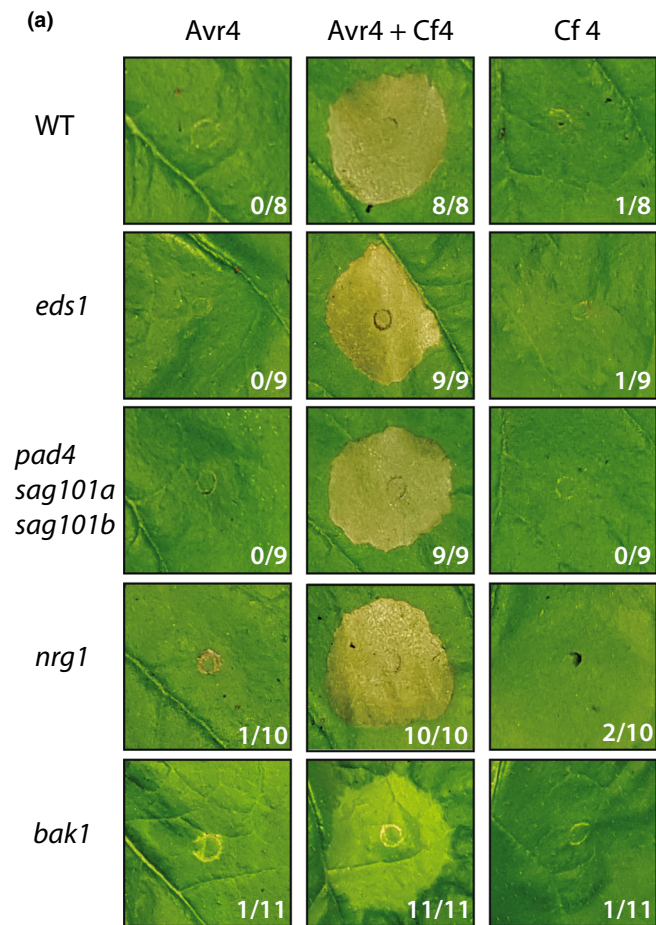


**Fig. 1** Receptor-like protein (RLP)- and receptor-like kinase (RLK)-mediated responses in *Nicotiana benthamiana* lines lacking Enhanced Disease Susceptibility 1 (EDS1) complexes or RPW8-type helper NLRs (RNLs) (NLR, nucleotide-binding domain leucine-rich repeat containing). (a) Cell death induction upon (co-)expression of Avr4 and Cf-4. Avr4 and/or Cf-4 were expressed by agroinfiltration ( $OD_{600} = 0.05$ ) in the indicated *N. benthamiana* (*Nb*) lines. Symptom (cell death) formation was documented 4 d postinfiltration (dpi). The experiment was conducted eight times with similar results, and representative images are shown. Numbers indicate infiltration sites with chlorosis (*bak1*, *Brassinosteroid-insensitive 1 (BRI1) Associated Kinase1*) or cell death (all remaining genotypes). (b) Quantitative assessment of cell death by ion leakage measurements. Leaf discs were sampled 24 h postinfiltration (hpi), washed for 2 h in  $H_2O$ , and incubated 24 h in  $H_2O$  under shaking before measuring conductivity. Three independent experiments, each conducted with four replicates, are shown and color-coded (red, green, blue). Horizontal line corresponds to the median, hinges indicate first and third quartiles and whiskers extend to the smallest/largest value or 1.5-fold the interquartile range. Letters indicate statistically significant differences (ANOVA, Tukey's honestly significant difference (HSD),  $P < 0.001$ ). (c) Avr4-induced reactive oxygen species (ROS) production in different *Nb* lines transiently expressing Cf-4 or  $\beta$ -glucuronidase (GUS, control). Leaves of indicated plant lines were used for transient expression of Cf-4 or GUS by agroinfiltration ( $OD_{600} = 0.1$ ). Leaf discs were elicited with Avr4 (100 nM) 3 d later, and ROS production was measured over 5 h. The area under the curve for 48 measurements from four independent experiments was plotted; mean and 95% CI are displayed.  $P$ -values for statistically significant differences are indicated (ANOVA, Dunnett's multiple comparison test). (d) flg22-induced production of reactive oxygen species (ROS) in different *Nb* lines. Leaf discs of 4 wk-old *Nb* plants of the indicated genotypes were treated with 2 nM flg22, and ROS production was measured over 60 min. The area under the curve for 64 measurements from four independent experiments was plotted; mean and 95% CI are displayed. Letters indicate statistically significant differences (ANOVA, Bonferroni *post hoc* test,  $P < 0.05$ ).

respective proteins from tomato (*S*) or *Nb* with XopQ (Gantner *et al.*, 2019; Lapin *et al.*, 2019). We used tomato proteins for functional interrogation, as previous EDS1 variants were generated in this context (Gantner *et al.*, 2019) and *S*EDS1 induces more robust cell death in transient complementation assays

compared to *Nb*EDS1. EDS1 family proteins from tomato and *Nb* are very similar (identity/similarity: EDS1 = 79%/86%; SAG101b = 72%/79%; Gantner *et al.*, 2019). In addition to cell death, EDS1-dependent pathogen resistance can be measured by mixed *Agrobacterium-Xcv* infections (Lapin *et al.*, 2019).

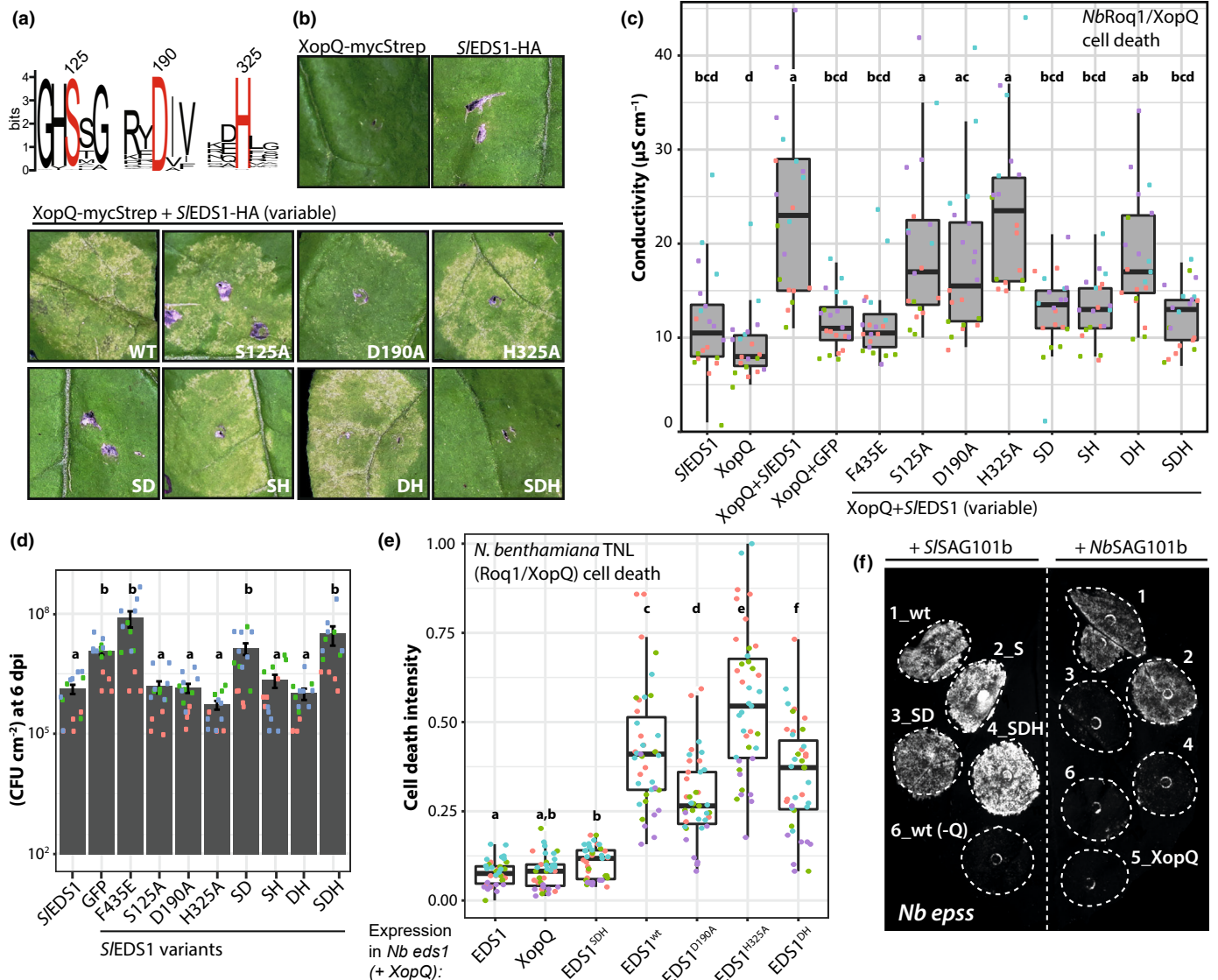


**Fig. 2** The tomato Enhanced Disease Susceptibility 1 (*S/EDS1*) catalytic triad is critical for *Xanthomonas* Outer Protein Q (XopQ)-induced cell death and pathogen resistance mediated by an *S/EDS1*-*NbsAG101b* complex in *Nicotiana benthamiana* (SAG101, Senescence Associated Gene 101). (a) Sequence logo of the predicted EDS1 catalytic triad positions generated from an alignment of 75 orthologous sequences. The triad S–D–H residues are highlighted, numbering corresponds to *S/EDS1*. EDS1 sequences from Lapin *et al.* (2019). (b) Cell death induction upon (co-)expression of XopQ and *S/EDS1*-variants as indicated. *Agrobacterium* strains for the expression of indicated proteins (under 35S promoter control) were infiltrated at OD<sub>600</sub> = 0.4 per strain into *N. benthamiana* (*Nb eds1* mutant plants. At 3 d postinfiltration (dpi), samples were taken for verification of protein expression (Fig. S6), and symptom (cell death) formation was documented 7 dpi. The experiment was conducted > 10 times with similar results, and representative images are shown. (c) Quantification of cell death by ion leakage measurements. Infiltrations and strains as in (b), but at 4 dpi, samples were taken for ion leakage measurements. The experiment was conducted four times with 4–6 replicates; independent experiments are color-coded. Horizontal line corresponds to the median, hinges indicate first and third quartiles and whiskers extend to the smallest/largest value or 1.5-fold the interquartile range. Letters indicate statistically significant differences (ANOVA, Tukey's honestly significant difference (HSD),  $P < 0.05$ ). (d) *Xanthomonas campestris* pv *vesicatoria* (*Xcv*) growth assay in *Nb eds1* plants transiently expressing GFP (green fluorescent protein, negative control), *S/EDS1* (positive control) or variants thereof, as indicated. Plants were co-infiltrated with *Agrobacterium* strains and *Xcv* bacteria, and *Xcv* bacterial titers determined 6 dpi. The experiment was conducted three times with 4–6 replicates. Individual data points are color-coded for experiments. Error bars represent SEM. Letters indicate statistically significant differences (ANOVA, Tukey's HSD,  $P < 0.05$ ). (e) Quantification of cell death by red light imaging. Graph shows composite data originating from four independent experiments. Per experiment, 7–12 leaves were used for agroinfiltration and documented 5 dpi. Cell death was quantified using IMAGEJ and normalized to a 0–1 range. Data from independent experiments are color-coded. Horizontal line corresponds to the median, hinges indicate first and third quartiles and whiskers extend to the smallest/largest value or 1.5-fold the interquartile range. Letters indicate statistically significant differences (ANOVA, Fisher's least significant difference (LSD),  $P < 0.05$ ). (f) XopQ-induced cell death mediated by *S/EDS1* or variants thereof in *Nb epss* plants with co-expression of *S/SAG101b* (left) or *NbsAG101b* (right). Proteins were expressed by agroinfiltration (OD<sub>600</sub> = 0.4 per strain) and cell death was visualized at 5 dpi by red light imaging. Abbreviations of used *S/EDS1* variants (wild-type (WT), S125A, SD, SDH) are indicated. As controls, XopQ was expressed alone (infiltration 5), and *S/EDS1* was co-expressed with *S/NbsAG101b* variants without XopQ (infiltration 6).

We generated *S*EDS1 variants with single or combined exchanges (to alanine) of the catalytic triad residues S125, D190 and H325. The *S*EDS1 variants were first tested in cell death assays by co-expression with XopQ in *Nb eds1* mutant plants (Fig. 2b). We consistently observed reduced TNL-triggered cell death upon co-expression of EDS1<sup>D190A</sup> with XopQ and cell death was abolished with EDS1<sup>SD</sup> or EDS1<sup>SDH</sup> (Fig. 2b). Exchange of the single S125 residue did not impair *S*EDS1 function. Remarkably, co-expression of H325 variants with XopQ induced mildly enhanced cell death (Fig. 2b; *S*EDS1 vs *S*EDS1<sup>H325A</sup> and *S*EDS1<sup>D190A</sup> vs *S*EDS1<sup>DH</sup>).

Quantification of cell death in ion leakage assays and testing of *S*EDS1 variants in *Xcv* resistance assays led to similar results: *S*EDS1<sup>SD</sup> and *S*EDS1<sup>SDH</sup> variants lost immune activity (Fig. 2c,d), similar to the nonfunctional *S*EDS1<sup>F435E</sup> variant (Gantner *et al.*, 2019). Minor macroscopic effects of *S*EDS1<sup>D190A</sup> and *S*EDS1<sup>H325A</sup> exchanges were not detected. Therefore, we quantified the intensity of cell death responses using red-light imaging (Landeo Villanueva *et al.*, 2021). Composite data from > 35 infiltrated leaves confirmed reduced and enhanced cell death intensities for *S*EDS1<sup>D190A</sup> and *S*EDS1<sup>H325A</sup>, respectively (Fig. 2e). Cell death strength did not correlate with differences in protein accumulation and *S*EDS1 variants formed a dimer with *S*SAG101b-Strep, as tested by co-purification (Fig. S6). Reduced levels of *S*EDS1<sup>SDH</sup> co-purified with Strep-tagged *S*SAG101b in most replicates (Fig. S6b). Levels of co-purified EDS1<sup>SDH</sup> exceeded those of *S*EDS1<sup>TIV</sup> (Fig. S6c), a variant carrying mutations in the hydrophobic  $\alpha$ H helix required for EDS1 stable interaction with SAG101 and functional in XopQ cell death assays (Gantner *et al.*, 2019). Thus, disruption of EDS1-SAG101 complexes or reduced stability of *S*EDS1 triad variants is unlikely to explain their immunity defects. However, it should be noted that cell death assays monitor activity of *S*EDS1 in complex with *Nb*SAG101b, whereas co-purification assays monitor interaction of *S*EDS1 with *S*SAG101b.

We conducted XopQ cell death assays in *Nb eds1* and *eps*s plants to test immune functions of *S*EDS1 together with *S*SAG101b and the effect of overexpression (OE) of *S*SAG101b or *Nb*SAG101b (Figs 2f, S7). *S*SAG101b-OE, but not *Nb*SAG101b-OE, enhanced cell death in XopQ assays in *eds1* plants (Fig. S7a,b). Under these conditions, the previously non-functional *S*EDS1<sup>SD</sup> and *S*EDS1<sup>SDH</sup> variants mediated cell death indistinguishable from that of WT *S*EDS1. Similarly, *S*EDS1<sup>SD</sup> and *S*EDS1<sup>SDH</sup> were functional upon *S*SAG101b-OE, but not *Nb*SAG101b-OE, in XopQ cell death assays in *eps*s plants (Fig. 2f). We also tested *S*EDS1 triad variants together with *S*SAG101b in cell death assays using the TIR domains of DM2h (Dangerous Mix 2 h; DM2h<sub>1-279</sub>) or RPS4 (Resistant to *Pseudomonas Syringae* 4; RPS4(E111K)<sub>1-234</sub>) as inducers (Gantner *et al.*, 2019). In these assays, *S*EDS1<sup>SD</sup> and *S*EDS1<sup>SDH</sup> (with *S*SAG101b-OE) mediated reduced cell death in approximately half of the tested leaves; no differences were observed for remaining leaves (Fig. S7c).

Overall, the results show that mutations within the *S*EDS1 catalytic triad can lead to reduced or enhanced immunity functions when *S*EDS1 integrates in heterologous complexes

together with *Nb*SAG101. Impaired immune functions of *S*EDS1<sup>SD/SDH</sup> variants (Fig. 2a-d) can be largely restored by *S*SAG101b-OE (Figs 2f, S7). Thus, triad residues may become critical only in the context of *S*EDS1 functioning with *Nb*SAG101b. Alternatively, reduced functionality of *S*EDS1<sup>SD/SDH</sup> could become masked by generally enhanced cell death upon *S*SAG101b-OE, as suggested by reduced cell death in some replicates when these variants were co-expressed with Arabidopsis TIR domains (Fig. S7c). However, TIR fragments induce generally weaker cell death than XopQ, which renders complementation assays less reliable.

### EDS1 protein catalytic triad residues are dispensable for immune signaling in Arabidopsis and *N. benthamiana*

Reduced immunity activities of *S*EDS1<sup>SD/SDH</sup> variants may result from confounding effects as a result of monitoring of their function in complex with *Nb*SAG101b. However, these observations might also be indicative of a previously overlooked function of the triad in immunity, possibly by small molecule binding. We investigated this hypothesis further.

First, we tested an extended set of triad variants of *At*EDS1-*At*PAD4 (Fig. 3). In earlier mutagenesis studies, *At*EDS1 variants including an SDH(FV) variant (further perturbation of the triad environment by F47W and V189M mutations) were functional in different TNL-ETI assays, and were tested together with *At*PAD4<sup>S118A</sup> and in presence of endogenous *At*SAG101 in Arabidopsis (Wagner *et al.*, 2013). We reasoned that partial disruption of the *At*PAD4 catalytic triad and/or *At*SAG101 presence might mask effects of exchanges within the *At*EDS1 catalytic triad.

We used three different approaches to test *At*EDS1-*At*PAD4 triad variants (Fig. 3a): (1) stable transformation of an Arabidopsis *eds1-12 pad4-1 sag101-3* triple mutant (*At eps*) with constructs encoding *At*EDS1 and *At*PAD4, and challenge of T<sub>1</sub> plants with *Hpa* Cala2 (resisted by RPP2 TNLs; Sinapidou *et al.*, 2004); (2) *Xcv*-Roq1 resistance assays in *Nb eps*s plants transiently expressing *At*NRG1.1, *At*SAG101 and *At*EDS1 by co-infiltration of plants with *Agrobacterium* strains and *Xcv* bacteria (Lapin *et al.*, 2019); and (3) Roq1 cell death assays by expressing XopQ with the same set of Arabidopsis proteins in *Nb eps*s plants, and ion leakage measurements (Lapin *et al.*, 2019).

In *At eps* plants, *Hpa* Cala2 resistance was restored by expression of *At*EDS1<sup>SDHFV</sup>-*At*PAD4<sup>SDH</sup> as efficiently as by the WT proteins (Fig. 3b). Likewise, *At*EDS1 variants were functional in heterologous *Nb* assays recording immune activities of the *At*EDS1-*At*SAG101 complex in *eps*s plants (Fig. 3c,d; the non-functional *At*EDS1<sup>F419E</sup> variant was included as control). In agreement with our earlier data (Wagner *et al.*, 2013), these data argue against a role of the catalytic triad of Arabidopsis EDS1 family proteins in TNL-ETI.

We considered whether the requirement for an intact catalytic triad could be specific for *S*EDS1, whereas *At*EDS1 might function by a different mechanism in Arabidopsis and *Nb*. Therefore, we tested functionality of *S*EDS1 and respective variants in stable transgenic Arabidopsis plants (Fig. 4). *S*EDS1 can

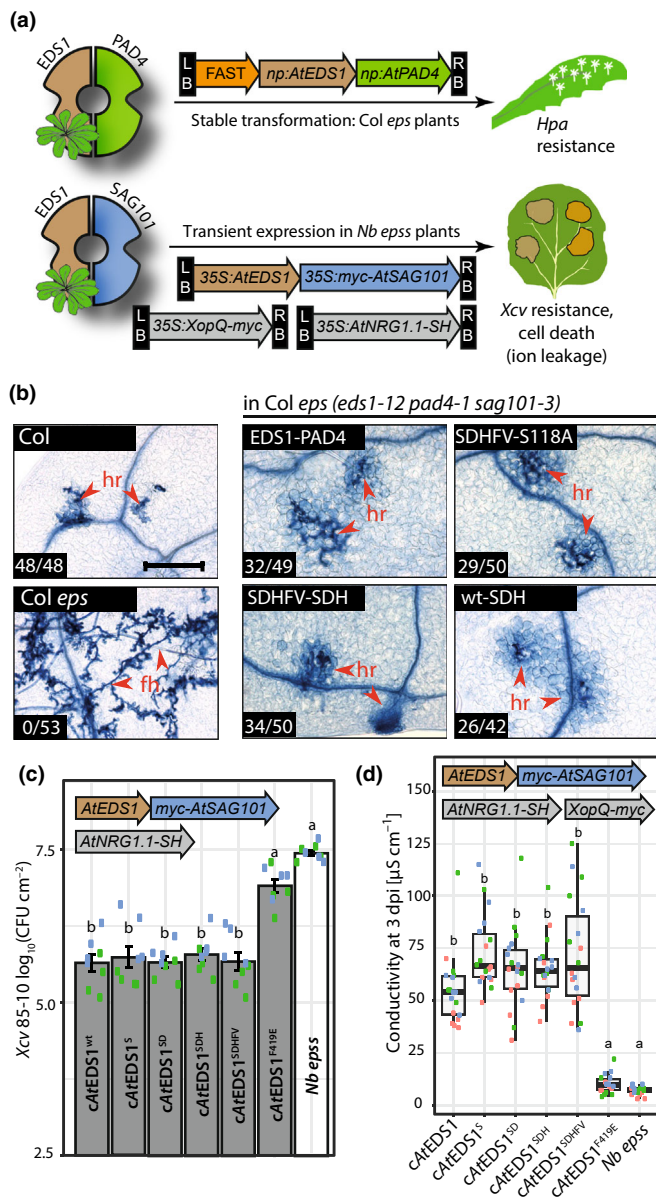


**Fig. 3** Immune signaling by *AtEDS1*-*AtPAD4* complexes does not depend on integrity of the catalytic triad. (a) Schematic depiction of used experimental setups to test functionality of Arabidopsis Enhanced Disease Susceptibility 1 (EDS1) family proteins in Arabidopsis (upper) and *Nicotiana benthamiana* (*Nb*; lower). Constructs coding for Arabidopsis EDS1-PAD4 (Phytoalexin-Deficient 4) and variants thereof, under native promoter control, were transformed into Arabidopsis plants deficient in EDS1 family proteins (*Col eps* = *eds1-12 pad4-1 sag101-3*). Resulting primary transformants were directly tested for resistance to *Hyaloperonospora arabidopsidis* (*Hpa*) isolate Cala2 (panel b). Constructs coding for Arabidopsis EDS1-SAG101 under 35S promoter control were used for transient expression in *Nb eps* mutant plants. Capacity of variants to mediate pathogen resistance was tested by mixed *Agrobacterium*-*Xanthomonas campestris* pv *vesicatoria* (*Xcv*) infiltrations with *Agrobacterium* strains harboring plasmids for expression of *AtEDS1* (or variants thereof), *AtSAG101* and *AtNRG1.1* (N-Required Gene 1) (panel c). Capacity of variants to mediate cell death was tested by co-expression with *AtSAG101*, *AtNRG1* and *XopQ*, and ion leakage measurements (panel d). (b) Infection of primary ( $T_1$ ) transformants and control lines with *Hpa* isolate Cala2. Primary transformants were selected by seed fluorescence. Three-wk-old plants were *Hpa*-infected, and first true leaves were used for Trypan Blue staining at 6 d postinfiltration (dpi). Numbers indicate the fraction of plants macroscopically scored as 'resistant' and the total number of analyzed plants. At least six primary transformants per construct were analyzed by Trypan Blue staining, and representative micrographs are shown. The experiment was conducted twice with similar results. Bar, 250  $\mu$ m. fh, free hyphae; hr, hypersensitive response. EDS1-SDHFV:S123A/D187A/H317A/F47W/V189M. PAD4-SDH:S118A/D178A/H229A. (c) Functionality of *AtEDS1* variants in *Xcv* resistance assays. Bacterial titers were determined 6 dpi. The experiment was conducted twice with four replicates in each experiment. Data points from individual experiments are color-coded. Error bars indicate SEM, letters statistically significant differences (ANOVA, Tukey's honestly significant difference (HSD),  $P < 0.001$ ). (d) Functionality of *AtEDS1* variants in cell death induction in *Nb*. Ion leakage was determined 3 dpi as quantitative measurement of cell death. The experiment was conducted three times with six replicate; data from independent experiments are color-coded. Horizontal line corresponds to the median, hinges indicate first and third quartiles and whiskers extend to the smallest/largest value or 1.5-fold the inter-quartile range. Statistics as in (c).

### Perturbation of the *S/EDS1* catalytic triad environment or lid region does not impair immune functions

We further queried the role of the *S/EDS1* catalytic triad environment and its predicted lid region in TNL-mediated immune responses. *AtEDS1* possesses an extended lid domain, composed of the helices  $\alpha$ F,  $\alpha$ G and  $\alpha$ H (Wagner *et al.*, 2013).  $\alpha$ G and  $\alpha$ H are in direct contact with PAD4 or SAG101 in complexes, whereas  $\alpha$ F lies across the entrance to a putative catalytic pocket (Fig. 5b). In GID1 (Gibberellin Insensitive Dwarf 1), the GA receptor, residues belonging to the core  $\alpha/\beta$ -hydrolase and the lid domain cooperate for substrate binding, and the lid region is critical for GA signaling (Shimada *et al.*, 2008; Rauwerdink & Kazlauskas, 2015). We targeted amino acids in the vicinity of the *S/EDS1* catalytic triad for mutagenesis (Figs 5a, S9; I214E, F235C, F235S, R194A, R194L, W58S, V192A, M195A, M195E, I210A and I214T), and generated two variants in which residues comprising helix  $\alpha$ F were deleted, and joined to  $\alpha$ G by a GGGG linker sequence (Fig. 5b; lid $\Delta$ #1:  $\Delta$ L206-P212, lid $\Delta$ #2:  $\Delta$ L207-S230). *S/EDS1* variants were co-expressed together with *XopQ* in *XopQ/Roq1* cell death assays in *Nb eds1* plants

function in Arabidopsis ETI when combined with *S/PAD4* (Gantner *et al.*, 2019; Lapin *et al.*, 2019). As before, different combinations of *S/EDS1* and *S/EDS1*<sup>SDH</sup> with *S/PAD4* or *S/PAD4*<sup>SDH</sup> (under control of Arabidopsis promoter fragments) were co-expressed in *At eps* plants. For each transformation, three to four independent transgenic lines were tested for resistance to *P. syringae* pv *tomato* DC3000 (*Pst*) *AvrRps4* that triggers the TNL receptor pair RPS4-RRS1 (Resistant to *Ralstonia Solanacearum* 1) (Narusaka *et al.*, 2009; Saucet *et al.*, 2015). Plants expressing the WT *S/EDS1*-*S/PAD4* construct almost fully restored RRS1-RPS4 resistance in the susceptible *At eps* mutant, as expected (Fig. 4b; Lapin *et al.*, 2019). All mutant variant constructs restored TNL resistance to the same extent as WT *S/EDS1*-*S/PAD4* (Figs 4b, S8). These experiments indicate that an intact catalytic triad is not required for immune activities of tomato EDS1 complexes in Arabidopsis TNL-ETI.



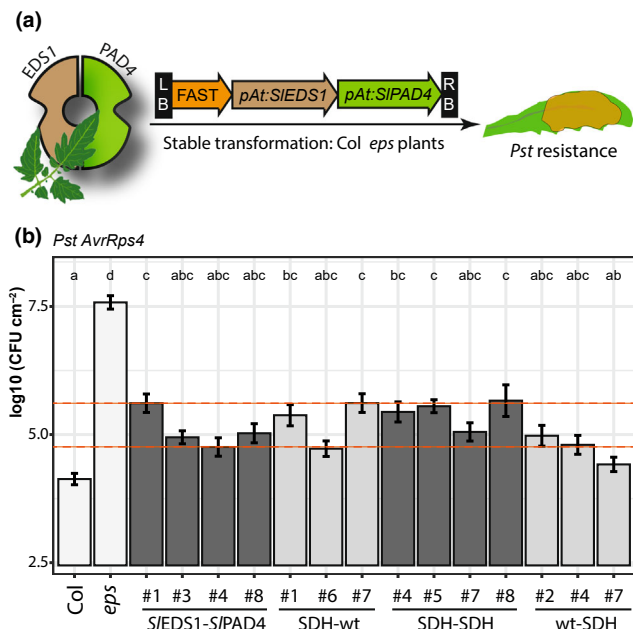


**Fig. 4** Integrity of the *S/EDS1-S/PAD4* catalytic triad is not critical for Arabidopsis TNL immunity. (a) Schematic depiction of experimental setup. Constructs coding for tomato *EDS1-PAD4* and variants thereof, under control of the respective Arabidopsis promoter elements, were transformed into Arabidopsis plants deficient in *EDS1* family proteins (*Col eps* = *eds1-12 pad4-1 sag101-3*). Resulting transformants were tested for resistance to *Pseudomonas syringae* (*Pst*) *AvrRps4* bacteria. (b) Resistance to *Pst AvrRps4* of transgenic lines expressing *S/EDS1-S/PAD4* or triad mutant variants thereof under control of Arabidopsis promoter elements in the *Col eps* mutant background. Transgenic segregants were selected by seed fluorescence (FAST marker) from *T*<sub>2</sub> populations. Four-wk-old plants were syringe-infiltrated with *Pst AvrRps4*, and bacterial titers were determined 3 d postinfiltration (dpi). At least three independent transgenic lines were tested per transformation, as indicated. Error bars represent SEM; graph shows composite data of three independent replicates (18 data points). Letters indicate statistically significant differences (ANOVA, Tukey's honestly significant difference (HSD), *P* < 0.05). Immunodetection of *S/EDS1-S/PAD4* proteins in transgenic lines is shown in Fig. S8.

(Fig. 5a). Astonishingly, all amino acid exchange variants and lid deletion variants mediated XopQ/Roq1 cell death as efficiently as WT *S/EDS1* (Figs 5c, S9). These data indicate that the *S/EDS1* triad environment and lid region are not necessary for immune signaling. Our results do not support small molecule binding to the *S/EDS1* catalytic triad region.

### Nuclear *EDS1* complexes are sufficient for XopQ/Roq1 cell death in *N. benthamiana*

We aimed to test in which subcellular compartment *S/EDS1-S/AG101b* complex activity is required for *Nb* TNL signaling. We generated constructs for expression of *S/EDS1*, *S/AG101b* or mis-localized variants, fused to yellow fluorescent protein (YFP; Fig. 6a). YFP-tagged *S/EDS1* or *S/AG101b* variants were transiently co-expressed with the respective mCherry-tagged complex partner in *Nb eps* quadruple mutant plants. When

monitoring functionality of *S/EDS1* and *S/AG101b* (cell death assays), XopQ was additionally co-expressed. Subcellular localization and accumulation of proteins were monitored at 3 d postinfiltration (dpi) by live cell imaging and immunodetection, respectively (Figs 6b, S10). Development of the XopQ/Roq1-induced cell death was documented 6 dpi (Fig. 6c).

For mislocalization, the fusion proteins were either decorated with a nuclear localization signal (e.g. *S/EDS1-YFP<sup>NLS</sup>*), a myristoylation motif (Myr-*S/EDS1-YFP*) or a nuclear export signal (*S/EDS1-YFP<sup>NES</sup>*). Attachment of a strong NLS was expected to deplete the cytosolic *S/EDS1-S/AG101b* pool by enhancing nuclear import (Fig. 6a; Garcia *et al.*, 2010; Stuttmann *et al.*, 2016). We used the classical SV40 NLS and that of c-myc, the human cancer protein. Similar results were obtained; only fusions containing the SV40-NLS are shown. The NES signal (from PKI; Wen *et al.*, 1995) mediates enhanced nuclear export but does not prevent nuclear import, and thus promotes shuttling between nucleus and cytoplasm and cytosolic accumulation (Fig. 6a; Garcia *et al.*, 2010). Attachment of a myristoylation motif was conducted to tether complexes to the plasma membrane, thus preventing cytosolic movement and nuclear import (Fig. 6a). Therefore, both NES and myristoylation motifs were expected to deplete nuclear protein pools. We used the myristoylation motifs of effectors HopZ2 and XopJ (Myr<sub>HopZ2</sub> and Myr<sub>XopJ</sub>), and generated G2A variants lacking a critical glycine residue as control (Lewis *et al.*, 2008; Bartetzko *et al.*, 2009). Similar results were obtained; we present only data using Myr<sub>XopJ</sub>(G2A) constructs. In two sets of experiments, *S/EDS1* (Fig. 6) or *S/AG101b* (Fig. S10) YFP fusions were mislocalized. Because stronger plant responses were obtained with the *S/EDS1-YFP* fusions, we continued assays with *S/EDS1-YFP* mis-localized forms.

As expected, transiently co-expressed *S/EDS1-YFP* and *S/AG101b-mCherry* complexes localized to the nucleus and cytoplasm (Fig. 6b; Gantner *et al.*, 2019), and were functional in XopQ/Roq1 cell death assays (Fig. 6c). When *S/EDS1-YFP<sup>NES</sup>* or fusions containing functional myristoylation motifs were expressed with *S/AG101b-YFP*, nuclear pools were diminished, because both *S/EDS1* and *S/AG101b* were detected mainly in the cytoplasm and at the nuclear periphery (NES) or plasma membrane (Myr; Fig. 6b). A G2A mutation in Myr<sub>XopJ</sub>(G2A)-*S/EDS1-YFP* restored nucleo-cytoplasmic distribution of *S/EDS1* and *S/AG101b* (Fig. 6b). Indeed, substantially reduced XopQ/Roq1 cell death was detected upon depletion of the nuclear *S/EDS1-S/AG101b* pool, and was restored upon co-expression of the Myr<sub>XopJ</sub>(G2A)-*S/EDS1-YFP* variant. By contrast, expression of *EDS1-YFP<sup>NLS</sup>* resulted in detection of *S/EDS1-S/AG101b* predominantly in the nucleus (Fig. 6b) and WT-like XopQ/Roq1 cell death induction (Fig. 6c). These results agree with earlier indications in Arabidopsis (Garcia *et al.*, 2010; Stuttmann *et al.*, 2016) that nuclear *EDS1* complexes are required and sufficient for TNL immunity. Nevertheless, we cannot exclude the possibility that low accumulation of the *EDS1-YFP<sup>NES</sup>* fusion (Fig. S10) or membrane tethering of Myr-*S/EDS1-YFP* interfere with protein function, beyond simply reducing its nuclear accumulation.

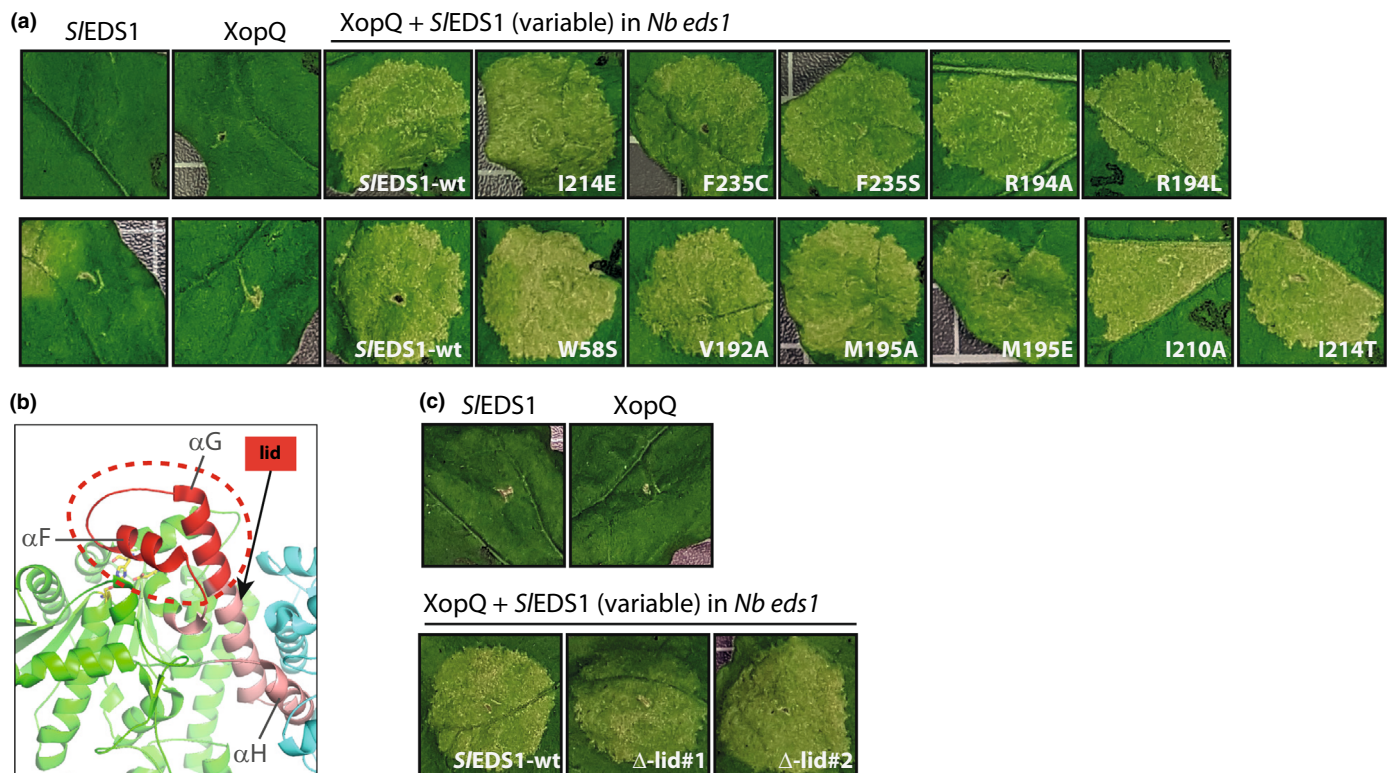


**Fig. 5** Perturbation of the *S/EDS1* (Enhanced Disease Susceptibility 1) catalytic triad environment. (a) Indicated single amino acid exchange variants of *S/EDS1* were co-expressed together with XopQ (*Xanthomonas* Outer Protein Q) in *Nicotiana benthamiana* (*Nb*) *eds1* mutant plants. XopQ/ Recognition Of XopQ 1 (Roq1)-mediated cell death was documented 6 dpi. The experiment was repeated at least five times with similar results, and representative images are shown. See also Fig. S9. (b) Schematic representation of *S/EDS1* lid deletions. In two different constructs, the section marked in red, or parts thereof, was replaced by a GGGG linker sequence. green,  $\alpha/\beta$  hydrolase core fold; cyan, SAG101b; pink, lid region and  $\alpha$ H helix; red, exposed lid region. (c) Lid deletions are functional in XopQ/Roq1 cell death assays. As in (a), but lid deletions were tested in cell death assays.

## Discussion

EDS1 complexes, together with ADR1- and NRG1-type hNLRs, form immunity signaling modules which in *Arabidopsis* are essential for TNL-initiated ETI and contribute to PTI signaling (Dongus & Parker, 2021). We demonstrate in *Nb* that EDS1-RNL modules are dispensable for several tested PTI responses (Fig. 1). Therefore, the role of EDS1 in complex with SAG101b appears to be more aligned with signal relay from activated receptors to RNLs in TNL immunity. We were intrigued by the observation that exchanges of lipase-like domain catalytic triad residues in immune-competent *S/EDS1* can enhance or abolish TNL immunity in *Nb* (Fig. 2), compatible with binding of TIR protein-derived small molecules to this region. However, this is limited to the situation in which *S/EDS1* functions together with *Nb*SAG101 in heterologous assays (Figs 2f, S7). Further in-depth analyses indicate that catalytic triad residues of EDS1 family proteins are not critical for immune signaling functions in *Arabidopsis* and *Nb* (Figs 2–4). Taken together with mutagenesis studies, including deletion of the *S/EDS1* lid region (Fig. 5), our data argue strongly against a contribution of the EDS1 N-terminal lipase pocket environment to immune signaling, beyond enabling dimer formation (Wagner *et al.*, 2013). Several mutational analyses pointed towards heterodimeric EDS1 complexes operating via

their conserved EP-domains (Gantner *et al.*, 2019; Lapin *et al.*, 2019; Dongus *et al.*, 2022). Indeed, TIR domain-derived NAD<sup>+</sup> ribosylation and hydrolysis products recently were identified buried in EP domain assemblies of EDS1-PAD4 and EDS1-SAG101 complexes (Huang *et al.*, 2022; Jia *et al.*, 2022). Specific small molecule binding led to a conformational change in the dimers which promoted their interaction with corresponding ADR1 and NRG1 hNLRs (Huang *et al.*, 2022; Jia *et al.*, 2022), that are assumed to then form membrane channels (Jacob *et al.*, 2021). Our data support an important function of *S/EDS1*-SAG101b complexes within the nucleus (Fig. 6). This prompts the question how and in which compartment RNLs are activated via EDS1 dimers.

## *N. benthamiana* LRR-RLK and LRR-RLP-mediated PTI and ETI-PTI connectivity

A dual role in plant development and immunity for SERK family LRR-RLKs is firmly established in different species (Chinchilla *et al.*, 2007; Fradin *et al.*, 2009; Chen *et al.*, 2014). In *Nb*, virus-induced gene silencing of *BAK1/SERK3*-like genes led to a strong reduction of the flg22-induced ROS burst response (measured with 50 nM flg22; Heese *et al.*, 2007). The *Nb bak1* mutant generated in this study displayed a reduced ROS burst when

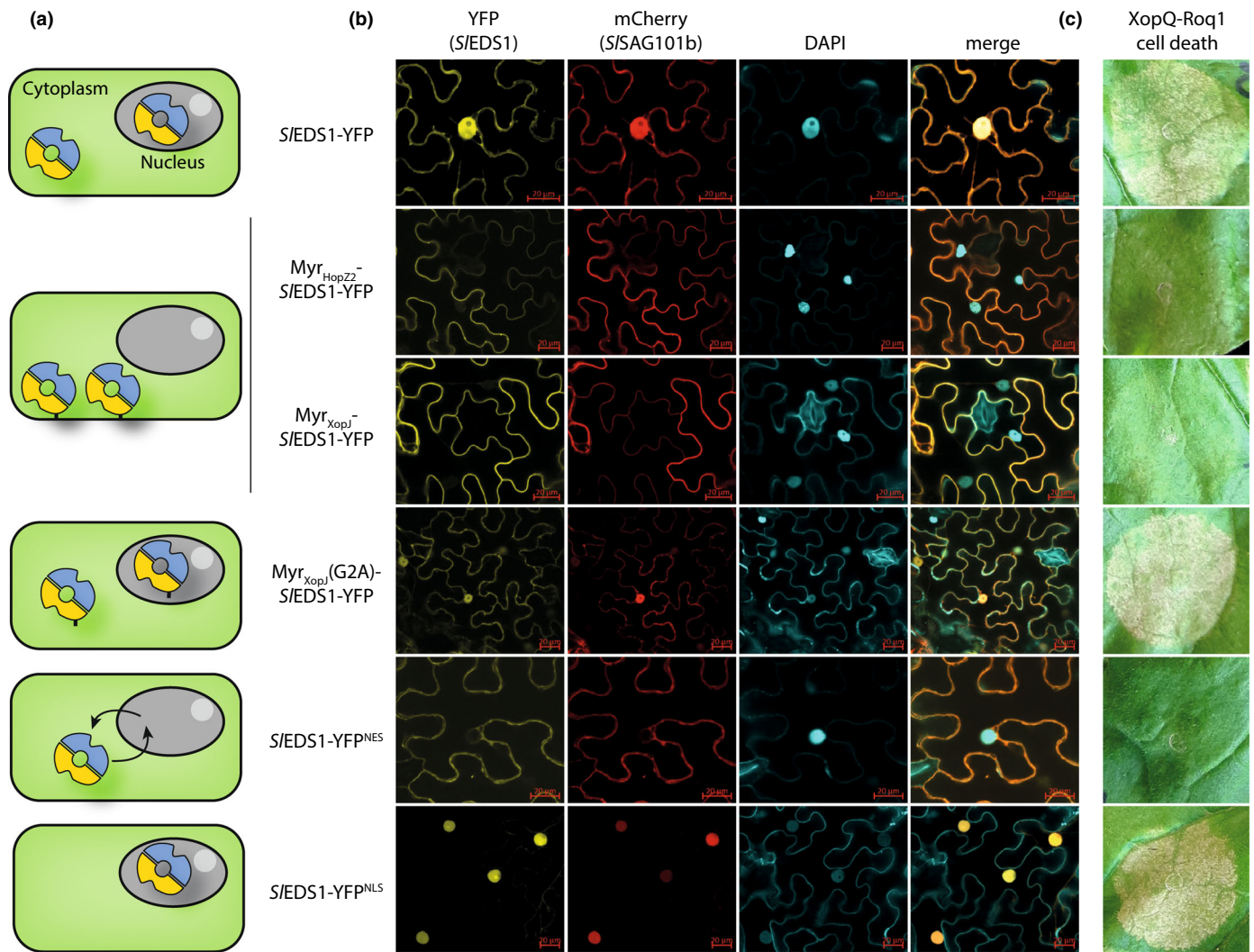


**Fig. 6** Immune-competence of mislocalized *S/EDS1* (Enhanced Disease Susceptibility 1) variants in *Nicotiana benthamiana* XopQ/Roq1 (Xanthomonas Outer Protein Q – Recognition Of Xop Q) cell death assays. (a) Scheme of modifications for mislocalization of *S/EDS1* complexes. *EDS1*-YFP without modifications is detected in nucleus and cytoplasm (Gantner *et al.*, 2019). YFP, yellow fluorescent protein. Myristoylation motifs tether *EDS1* and also *SAG101b* (Senescence Associated Gene 101) to the membrane. The G2A mutation abolishes myristoylation. Nuclear export signals (NES) leads to export from the nucleus, but does not prevent import, leading to import/export cycles and enhanced cytoplasmic accumulation. Nuclear localization signal (NLS) facilitate enhanced import. (b) Live cell imaging of (mislocalized) *S/EDS1*-*S/SAG101b* expressed by agroinfiltration in *N. benthamiana* (*Nb*) *epss* plants. All images show single planes, and micrographs were taken 3 d postinfiltration (dpi). Localizations were determined for three independent experiments. Representative micrographs from expression of indicated proteins without XopQ are shown. Similar results were obtained upon Xop co-expression, but with reduced fluorescence intensities. Protein accumulation of variants is shown in Fig. S10(a). Bar, 20 μm. (c) Cell death signaling by mislocalized *S/EDS1*-*S/SAG101b*(mCherry) complexes with XopQ in *Nb epss* plants was documented 6 dpi. Cell death phenotypes were assessed in five independent experiments with similar results.

challenged with 2 nM flg22, but was indistinguishable from the WT with a higher ligand concentration (Figs 1, S1–S4). These differences suggest that additional *SERK* family genes, silenced by VIGS but not inactivated in the *Nb bak1* double mutant, contribute to *Nb* PTI signaling. Indeed, the *Nb* genome (<https://www.nbentham.com/>; v.3.5) encodes four protein orthologs most similar to *AtBAK1* (Table S1). Respective mRNAs have extensive similarity to the silencing construct used by Heese *et al.* (2007). It is therefore plausible that the two further *BAK1*-like genes not targeted for mutagenesis mediate LRR-RLK and LRR-RLP responses in the *Nb bak1* mutant line. Further *SERK* family genes

might also contribute to *Nb* PTI signaling (Fradin *et al.*, 2011; Postma *et al.*, 2016).

PTI assays with low inoculum densities (Avr4/9) and elicitor concentrations (Avr4, flg22) allowed detection of weakly impaired PTI in *Nb bak1*, whereas *eds1* or *rnl* mutant lines behaved like the WT in the same experiments (Figs 1, S3). These results suggest that RLP- and RLK-mediated responses, as far as tested, do not require an intact TNL signaling sector in *Nb*. Recruitment of *EDS1*-*RNL* modules for PTI signaling (Pruitt *et al.*, 2021; Tian *et al.*, 2021) might thus represent a derived function of these TNL immune sector components in

Arabidopsis and potentially other Brassicaceae species. Alternatively, EDS1-RNL modules in *Nb* could support signaling by surface receptors not analyzed here and/or promote a different set of signaling outputs.

Intriguingly, hNLRs of the NRC superclade, in particular NRC3, were found to be required for cell death initiated by Cf4/Avr4 and further LRR-RPs in *Nb* (Gabriels *et al.*, 2006, 2007; Fradin *et al.*, 2009; Kourelis *et al.*, 2021). Therefore, dependency of cell surface receptor signaling on intracellular NLR networks might be a conserved property but executed by diverse mechanisms for different receptors or particular plant species, in agreement with large structural and functional diversity observed among both surface-localized as well as intracellular immune receptors (Zipfel, 2014; Van de Weyer *et al.*, 2019; Lu & Tsuda, 2021; Pruitt *et al.*, 2021). Notably, PTI-ETI connections might correlate with evolutionary trajectories and expansions of specific immune sectors in species: whereas Arabidopsis has a large number of TNLs, *Nb* has relatively few TNLs but expanded NRCs (Hofberger *et al.*, 2014; Wu *et al.*, 2017; Johannndrees *et al.*, 2021).

### Role of EDS1 complexes in TNL immunity signaling

A core function of EDS1 complexes is in signal transmission from activated TNL-type immune receptors to RNL-type hNLRs. TIR domains of bacterial, plant and animal origins, including the full-length TNLs RPP1 and Roq1, were recognized as NAD<sup>+</sup>-consuming enzymes (Essuman *et al.*, 2017, 2018; Horsefield *et al.*, 2019; Wan *et al.*, 2019; Ma *et al.*, 2020; Martin *et al.*, 2020; Ofir *et al.*, 2021). Depletion of NAD<sup>+</sup> by a TIR-domain protein initiates axon degeneration, a neuronal self-destruction program, in animals (Essuman *et al.*, 2017). A mechanism in which one or several products of TIR enzymatic activities function as signal intermediates is more likely in TNL immunity, because isolated (TNL) TIR domains which are sufficient to induce cell death, demonstrate comparably low NADase activity and do not deplete cellular NAD<sup>+</sup> stores. Also, NADase activity is not sufficient for TNL signaling (Wan *et al.*, 2019; Duxbury *et al.*, 2020). Recently, a number of NAD isomers were identified as TIR domain enzymatic products (Huang *et al.*, 2022; Jia *et al.*, 2022; Leavitt *et al.*, 2022; Manik *et al.*, 2022). Amongst these, pRib-ADP/AMP and ADPr-ATP were found buried within the EP domain assemblies of Arabidopsis EDS1-PAD4 and EDS1-SAG101 complexes, respectively, and promote interactions with corresponding hNLRs (Huang *et al.*, 2022; Jia *et al.*, 2022).

Intrigued by impaired immune functions of S/EDS1<sup>SD/SDH</sup>, but not S/EDS1<sup>S125A</sup> in *Nb* (Fig. 2; when in complex with NbSAG101b), we used mutagenesis studies to probe small molecule binding to an alternative candidate site, the conserved catalytic triad and assumed substrate binding pocket of EDS1 proteins. The triad environment could serve for binding of yet another NAD isomer or a different molecule to fine-tune or control complex activity in a dual-gating mechanism. However, catalytic triad residues only became relevant in the context of a heterologous S/EDS1-NbSAG101b complex (Figs 2f, 3–5, S7).

This also should be taken as a note of caution that, despite the high similarity between the proteins from *Sl* and *Nb*, there can be functional barriers.

We assume that these in-depth analyses allow us to dismiss the triad environment as a candidate region for small molecule binding in Arabidopsis and *Nb* immunity (Figs 2–5). Also, we show that the S/EDS1 lid region is dispensable for at least TNL-ETI in *Nb* (Fig. 5). This was tested to explore possible functional analogy to the  $\alpha/\beta$ -hydrolase-based small molecule receptors GID1 and D14 (Dwarf14), which recruit interactors in a ligand-dependent manner via their lid domains (Mindrebo *et al.*, 2016; Seto *et al.*, 2019). Thus, beyond providing a structural scaffold for alignment of EP domains, the EDS1 complex N-terminal lipase domain assemblies most likely not contribute to TNL-ETI. This is supported by an AF2 model of the ternary EDS1-SAG101-NRG1 complex from Arabidopsis (Fig. S5e), in which NRG1 does not make contacts with the lipase-like domains of either EDS1 or SAG101. Functions of EDS1 family lipase-like domains and triad residues, despite strong conservation, thus so far remain limited to a role in Arabidopsis PAD4-mediated resistance to green peach aphid infestation (Louis *et al.*, 2012; Dongus *et al.*, 2020).

### Subcellular compartmentalization of TNL immune signal relay in *N. benthamiana*

TNL activation and signaling involves small molecule production via TIR-NADase and/or TIR-2',3'-cAMP/cGMP synthetase activities (Horsefield *et al.*, 2019; Wan *et al.*, 2019; Huang *et al.*, 2022; Jia *et al.*, 2022; Leavitt *et al.*, 2022; Manik *et al.*, 2022; Yu *et al.*, 2022). TIR-derived small molecules can be expected to be mobile within the cell, and could therefore be produced in different subcellular compartments in alignment with immune receptor localization and function. Indeed, subcellular localizations including nucleus, plasma membrane and endomembrane systems were reported for TNLs (e.g. Takemoto *et al.*, 2012). However, the TNLs N (from *N. tabacum*) and RPS4 (from Arabidopsis) localize within the nucleus for effective TNL immunity (Burch-Smith *et al.*, 2007; Wirthmueller *et al.*, 2007; Huh *et al.*, 2017). Similarly, nuclear EDS1 complexes are sufficient for natural pathogen resistance and TNL autoimmunity in Arabidopsis, whereas nuclear exclusion impairs TNL immune responses (Garcia *et al.*, 2010; Stuttmann *et al.*, 2016; Cui *et al.*, 2018; Ordon *et al.*, 2021). The subcellular localization of *Nb* Roq1 and site of XopQ recognition were so far not reported. Results presented here from mis-localizing S/EDS1-S/EDS101b complexes suggest that activation of EDS1 complexes inside nuclei is sufficient and also critical for Roq1 cell death signaling in *Nb* (Fig. 6).

Activated forms of RNL-type hNLRs NRG1 and ADR1, functioning downstream or together with EDS1 complexes in Arabidopsis and *Nb*, were reported to localize to the plasma membrane, endoplasmatic reticulum membrane and the cytosol (Wu *et al.*, 2018; Lapin *et al.*, 2019; Jacob *et al.*, 2021; Saile *et al.*, 2021). In the case of *At*ADR1, counteracting plasma membrane localization by depletion of phosphatidylinositol-4-

phosphate impaired ADR1-mediated cell death induction, further supporting membrane-associated functions of ADR1 in immunity (Saile *et al.*, 2021). Recently, also nuclear localization and functions of Arabidopsis NRG1 were proposed (Feehan *et al.*, 2022), and appear not to be linked to NRG1 resistosome formation (Feehan *et al.*, 2022). It is of major interest for future analyses to determine how and in which compartment EDS1-RNL interactions (Qi *et al.*, 2018; Sun *et al.*, 2021; Wu *et al.*, 2021) mediate RNL activation and TNL immunity.

## Acknowledgements

This work was funded by GRC grant STU 642-1/1 (Deutsche Forschungsgemeinschaft, DFG) to JS. Furthermore, JS is grateful for support through the Leibniz price from the DFG and the Alfred Krupp von Bohlen und Halbach Stiftung, awarded to Ulla Bonas. DL and JEP acknowledge support from The Max-Planck Society and Deutsche Forschungsgemeinschaft (DFG, German Research Foundation) SFB-1403-414786233. SLV was financed by the Peruvian Council for Science, Technology and Technological Innovation (CONCYTEC) and its executive unit FONDECYT. We are grateful to Bianca Rosinsky for taking care of plant growth facilities and growing plants. We thank Bart Thomma for providing Avr4/Cf4 and Avr9/Cf9 expression constructs and Sebastian Schornack for discussion of BAK1 orthologs.

## Author contributions

JZ, JG, DL, KB, LEL, SZ, JLE and CK performed experiments and analyzed data; JZ, DL, KB and LEL contributed to figure preparation; SLV and MHAJJ contributed Cf4 ROS data; RG performed molecular modeling and structural analyses; JS conceptualized and supervised work, performed experiments and analyzed data, prepared figures, and wrote the manuscript with contributions from DL and JEP; and all authors approved the final version. JZ, JG and DL contributed equally to this work.

## ORCID

Karen Barthel  <https://orcid.org/0000-0002-3753-0561>  
 Jessica L. Erickson  <https://orcid.org/0000-0002-7713-6366>  
 Lennart Eschen-Lippold  <https://orcid.org/0000-0001-8907-6922>  
 Johannes Gantner  <https://orcid.org/0000-0003-3961-8660>  
 Raphael Guerois  <https://orcid.org/0000-0001-5294-2858>  
 Matthieu H. A. J. Joosten  <https://orcid.org/0000-0002-6243-4547>  
 Carola Kretschmer  <https://orcid.org/0000-0001-7315-7840>  
 Dmitry Lapin  <https://orcid.org/0000-0001-9591-3950>  
 Jane E. Parker  <https://orcid.org/0000-0002-4700-6480>  
 Johannes Stuttmann  <https://orcid.org/0000-0002-6207-094X>  
 Sergio Landeo Villanueva  <https://orcid.org/0000-0001-7521-4765>  
 Josua Zönnchen  <https://orcid.org/0000-0002-5427-896X>  
 Stefan Zantop  <https://orcid.org/0000-0002-5799-6801>

## Data availability

The data that support the findings of this study are available within the article and Supporting Information. ALPHAFOLD2 models were deposited in ModelArchive ([www.modelarchive.org](http://www.modelarchive.org)) with identifiers ma-k5om5 (*A#EDS1-A#SAG101*), ma-ewx53 (*A#EDS1-A#SAG101-A#NRG1*) and ma-cf7k5 (*S#EDS1-S#SAG101*).

## References

- Adlung N, Prochaska H, Thieme S, Banik A, Blüher D, John P, Nagel O, Schulze S, Gantner J, Delker C *et al.* 2016. Non-host resistance induced by the *Xanthomonas* effector XopQ is widespread within the genus *Nicotiana* and functionally depends on EDS1. *Frontiers in Plant Science* 7: 1796.
- Baggs EL, Monroe JG, Thanki AS, O'Grady R, Schudoma C, Haerty W, Krasileva KV. 2020. Convergent loss of an EDS1/PAD4 signaling pathway in several plant lineages reveals coevolved components of plant immunity and drought response. *Plant Cell* 32: 2158–2177.
- Barragan AC, Weigel D. 2021. Plant NLR diversity: the known unknowns of pan-NLRomes. *Plant Cell* 33: 814–831.
- Bartetzko V, Sonnwald S, Vogel F, Hartner K, Stadler R, Hammes UZ, Bornke F. 2009. The *Xanthomonas campestris* pv. *vesicatoria* type III effector protein XopJ inhibits protein secretion: evidence for interference with cell wall-associated defense responses. *Molecular Plant–Microbe Interactions* 22: 655–664.
- Bentham A, Burdett H, Anderson PA, Williams SJ, Kobe B. 2017. Animal NLRs provide structural insights into plant NLR function. *Annals of Botany* 119: 827–702.
- Bernoux M, Zetzsche H, Stuttmann J. 2022. Connecting the dots between cell surface- and intracellular-triggered immune pathways in plants. *Current Opinion in Plant Biology* 69: 102276.
- Bhandari DD, Lapin D, Kracher B, von Born P, Bautor J, Niefind K, Parker JE. 2019. An EDS1 heterodimer signalling surface enforces timely reprogramming of immunity genes in Arabidopsis. *Nature Communications* 10: 772.
- Bi G, Su M, Li N, Liang Y, Dang S, Xu J, Hu M, Wang J, Zou M, Deng Y *et al.* 2021. The ZAR1 resistosome is a calcium-permeable channel triggering plant immune signaling. *Cell* 184: 3528–3541.
- Bonardi V, Tang S, Stallmann A, Roberts M, Cherkis K, Dangl JL. 2011. Expanded functions for a family of plant intracellular immune receptors beyond specific recognition of pathogen effectors. *Proceedings of the National Academy of Sciences, USA* 108: 16463–16468.
- Burch-Smith TM, Schiff M, Caplan JL, Tsao J, Czymbek K, Dinesh-Kumar SP. 2007. A novel role for the TIR domain in association with pathogen-derived elicitors. *PLoS Biology* 5: e68.
- Castel B, Ngou PM, Cevik V, Redkar A, Kim DS, Yang Y, Ding P, Jones JDG. 2018. Diverse NLR immune receptors activate defence via the RPW8-NLR NRG1. *New Phytologist* 222: 966–980.
- Chen X, Zuo S, Schwessinger B, Chern M, Canlas PE, Ruan D, Zhou X, Wang J, Daudi A, Petzold CJ *et al.* 2014. An XA21-associated kinase (OsSERK2) regulates immunity mediated by the XA21 and XA3 immune receptors. *Molecular Plant* 7: 874–892.
- Chinchilla D, Zipfel C, Robatzek S, Kemmerling B, Nurnberger T, Jones JD, Felix G, Boller T. 2007. A flagellin-induced complex of the receptor FLS2 and BAK1 initiates plant defence. *Nature* 448: 497–500.
- Collier SM, Hamel LP, Moffett P. 2011. Cell death mediated by the N-terminal domains of a unique and highly conserved class of NB-LRR protein. *Molecular Plant–Microbe Interactions* 24: 918–931.
- Cui H, Qiu J, Zhou Y, Bhandari DD, Zhao C, Bautor J, Parker JE. 2018. Antagonism of transcription factor MYC2 by EDS1/PAD4 complexes bolsters salicylic acid defense in Arabidopsis effector-triggered immunity. *Molecular Plant* 11: 1053–1066.
- Cui H, Tsuda K, Parker JE. 2015. Effector-triggered immunity: from pathogen perception to robust defense. *Annual Review of Plant Biology* 66: 487–511.

- Dongus JA, Bhandari DD, Patel M, Archer L, Dijkgraaf L, Deslandes L, Shah J, Parker JE. 2020. The Arabidopsis PAD4 lipase-like domain is sufficient for resistance to green peach aphid. *Molecular Plant–Microbe Interactions* 33: 328–335.
- Dongus JA, Bhandari DD, Penner E, Lapin D, Stolze SC, Harzen A, Patel M, Archer L, Dijkgraaf L, Shah J *et al.* 2022. Cavity surface residues of PAD4 and SAG101 contribute to EDS1 dimer signaling specificity in plant immunity. *The Plant Journal* 110: 1415–1432.
- Dongus JA, Parker JE. 2021. EDS1 signalling: at the nexus of intracellular and surface receptor immunity. *Current Opinion in Plant Biology* 62: 102039.
- Duxbury Z, Wang S, MacKenzie CI, Tenthorpe JL, Zhang X, Huh SU, Hu L, Hill L, Ngou PM, Ding P *et al.* 2020. Induced proximity of a TIR signaling domain on a plant-mammalian NLR chimera activates defense in plants. *Proceedings of the National Academy of Sciences, USA* 117: 18832–18839.
- Engler C, Youles M, Gruetznr R, Ehnert TM, Werner S, Jones JD, Patron NJ, Marillonnet S. 2014. A golden gate modular cloning toolbox for plants. *ACS Synthetic Biology* 3: 839–843.
- Essuman K, Summers DW, Sasaki Y, Mao X, Yim AKY, DiAntonio A, Milbrandt J. 2018. TIR domain proteins are an ancient family of NAD<sup>+</sup>-consuming enzymes. *Current Biology* 28: 421–430.
- Essuman K, Summers DW, Sasaki Y, Mao XR, DiAntonio A, Milbrandt J. 2017. The SARM1 Toll/Interleukin-1 receptor domain possesses intrinsic NAD<sup>+</sup> cleavage activity that promotes pathological axonal degeneration. *Neuron* 93: 1334–1343.
- Feehan JM, Wang J, Sun X, Choi J, Ahn H-K, Ngou BPM, Parker JE, Jones JDG. 2022. Oligomerisation of a plant helper NLR requires cell-surface and intracellular immune receptor activation. *bioRxiv*. doi: 10.1101/2022.06.16.496440.
- Fradin EF, Abd-El-Halim A, Masini L, van den Berg GC, Joosten MH, Thomma BP. 2011. Interfamily transfer of tomato *Ve1* mediates *Verticillium* resistance in Arabidopsis. *Plant Physiology* 156: 2255–2265.
- Fradin EF, Zhang Z, Juarez Ayala JC, Castroverde CD, Nazar RN, Robb J, Liu CM, Thomma BP. 2009. Genetic dissection of *Verticillium* wilt resistance mediated by tomato *Ve1*. *Plant Physiology* 150: 320–332.
- Gabriels SH, Takken FL, Vossen JH, de Jong CF, Liu Q, Turk SC, Wachowski LK, Peters J, Witsenboer HM, de Wit PJ *et al.* 2006. cDNA-AFLP combined with functional analysis reveals novel genes involved in the hypersensitive response. *Molecular Plant–Microbe Interactions* 19: 567–576.
- Gabriels SHEJ, Vossen JH, Ekengren SK, van Ooijen G, Abd-El-Halim AM, van den Berg GCM, Rainey DY, Martin GB, Takken FLW, de Wit PJGM *et al.* 2007. An NB-LRR protein required for HR signalling mediated by both extra- and intracellular resistance proteins. *The Plant Journal* 50: 14–28.
- Gantner J, Ordon J, Ilse T, Kretschmer C, Gruetznr R, Lofke C, Dagdaz Y, Burstenbinder K, Marillonnet S, Stuttmann J. 2018. Peripheral infrastructure vectors and an extended set of plant parts for the modular cloning system. *PLoS ONE* 13: e0197185.
- Gantner J, Ordon J, Kretschmer C, Guerois R, Stuttmann J. 2019. An EDS1-SAG101 complex is essential for TNL-mediated immunity in *Nicotiana benthamiana*. *Plant Cell* 31: 2456–2474.
- Garcia AV, Blanvillain-Baufume S, Huibers RP, Wiermer M, Li G, Gobbato E, Rietz S, Parker JE. 2010. Balanced nuclear and cytoplasmic activities of EDS1 are required for a complete plant innate immune response. *PLoS Pathogens* 6: e1000970.
- Goldman A, Harper S, Speicher DW. 2016. Detection of proteins on blot membranes. *Current Protocols in Protein Science* 86: 10.8.1–10.8.11.
- Gomez-Gomez L, Felix G, Boller T. 1999. A single locus determines sensitivity to bacterial flagellin in *Arabidopsis thaliana*. *The Plant Journal* 18: 277–284.
- Heese A, Hann DR, Gimenez-Ibanez S, Jones AM, He K, Li J, Schroeder JI, Peck SC, Rathjen JP. 2007. The receptor-like kinase SERK3/BAK1 is a central regulator of innate immunity in plants. *Proceedings of the National Academy of Sciences, USA* 104: 12217–12222.
- Hofberger JA, Zhou B, Tang H, Jones JD, Schranz ME. 2014. A novel approach for multi-domain and multi-gene family identification provides insights into evolutionary dynamics of disease resistance genes in core eudicot plants. *BMC Genomics* 15: 966.
- Horsefield S, Burdett H, Zhang XX, Manik MK, Shi Y, Chen J, Qi TC, Gilley J, Lai JS, Rank MX *et al.* 2019. NAD<sup>+</sup> cleavage activity by animal and plant TIR domains in cell death pathways. *Science* 365: 793–799.
- Hu G, deHart AK, Li Y, Ustach C, Handley V, Navarre R, Hwang CF, Aegerter BJ, Williamson VM, Baker B. 2005. *EDS1* in tomato is required for resistance mediated by TIR-class R genes and the receptor-like R gene *Ve*. *The Plant Journal* 42: 376–391.
- Huang S, Jia A, Song W, Hessler G, Meng Y, Sun Y, Xu L, Laessle H, Jirschtzka J, Ma S *et al.* 2022. Identification and receptor mechanism of TIR-catalyzed small molecules in plant immunity. *Science* 377: eabq3297.
- Huh SU, Cevik V, Ding P, Duxbury Z, Ma Y, Tomlinson L, Sarris PF, Jones JDG. 2017. Protein–protein interactions in the RPS4/RRS1 immune receptor complex. *PLoS Pathogens* 13: e1006376.
- Jacob P, Kim NH, Wu F, El-Kasbi F, Chi Y, Walton WG, Furzer OJ, Lietzan AD, Sunil S, Kempthorn K *et al.* 2021. Plant “helper” immune receptors are Ca<sup>2+</sup>-permeable nonselective cation channels. *Science* 373: 420–425.
- Jia A, Huang S, Song W, Wang J, Meng Y, Sun Y, Xu L, Laessle H, Jirschtzka J, Hou J *et al.* 2022. TIR-catalyzed ADP-ribosylation reactions produce signaling molecules for plant immunity. *Science* 377: eabq8180.
- Johannndrees O, Baggs EL, Uhlmann C, Locci F, Läßle HL, Melkonian K, Käufer K, Dongus JA, Nakagami H, Krasileva KV *et al.* 2021. Differential *EDS1* requirement for cell death activities of plant TIR-domain proteins. *bioRxiv*. doi: 10.1101/2021.11.29.470438.
- Jumper J, Evans R, Pritzel A, Green T, Figurnov M, Ronneberger O, Tunyasuvunakool K, Bates R, Židek A, Potapenko A *et al.* 2021. Highly accurate protein structure prediction with ALPHAFOLD. *Nature* 596: 583–589.
- Kourelis J, Contreras MP, Harant A, Adachi H, Derevnina L, Wu C-H, Kamoun S. 2021. The helper NLR immune protein NRC3 mediates the hypersensitive cell death caused by the cell-surface receptor Cf-4. *bioRxiv*. doi: 10.1101/2021.09.28.461843.
- Landeo Villanueva S, Malvestiti MC, van Ieperen W, Joosten M, van Kan JAL. 2021. Red light imaging for programmed cell death visualization and quantification in plant–pathogen interactions. *Molecular Plant Pathology* 22: 361–372.
- Lapin D, Bhandari DD, Parker JE. 2020. Origins and immunity networking functions of EDS1 family proteins. *Annual Review of Phytopathology* 58: 253–276.
- Lapin D, Kovacova V, Sun X, Dongus JA, Bhandari DD, von Born P, Bautor J, Guarneri N, Rzemieniewski J, Stuttmann J *et al.* 2019. A coevolved EDS1-SAG101-NRG1 module mediates cell death signaling by TIR-domain immune receptors. *Plant Cell* 31: 2430–2455.
- Leavitt A, Yirmiya E, Amitai G, Lu A, Garb J, Herbst E, Morehouse BR, Hobbs SJ, Antine SP, Sun Z-YJ, Kranzusch PJ, Sorek R. 2022. Viruses inhibit TIR gcADPR signaling to overcome bacterial defense. *Nature* 2022. doi: 10.1038/s41586-022-05375-9.
- Lewis JD, Abada W, Ma W, Guttman DS, Desveaux D. 2008. The HopZ family of *Pseudomonas syringae* type III effectors require myristoylation for virulence and avirulence functions in *Arabidopsis thaliana*. *Journal of Bacteriology* 190: 2880–2891.
- Liebrand TW, van den Berg GC, Zhang Z, Smit P, Cordewener JH, America AH, Sklenar J, Jones AM, Tameling WI, Robatzek S *et al.* 2013. Receptor-like kinase SOBIR1/EVR interacts with receptor-like proteins in plant immunity against fungal infection. *Proceedings of the National Academy of Sciences, USA* 110: 10010–10015.
- Liu Y, Zeng Z, Zhang Y-M, Li Q, Jiang X-M, Jiang Z, Tang J-H, Chen D, Wang Q, Chen J-Q *et al.* 2021. An angiosperm NLR Atlas reveals that NLR gene reduction is associated with ecological specialization and signal transduction component deletion. *Molecular Plant* 14: 2015–2031.
- Logemann E, Birkenbihl RP, Ulker B, Somssich IE. 2006. An improved method for preparing Agrobacterium cells that simplifies the Arabidopsis transformation protocol. *Plant Methods* 2: 16.
- Louis J, Gobbato E, Mondal HA, Feys BJ, Parker JE, Shah J. 2012. Discrimination of Arabidopsis PAD4 activities in defense against green peach aphid and pathogens. *Plant Physiology* 158: 1860–1872.
- Lu Y, Tsuda K. 2021. Intimate association of PRR- and NLR-mediated signaling in plant immunity. *Molecular Plant–Microbe Interactions* 34: 3–14.
- Ma S, Lapin D, Liu L, Sun Y, Song W, Zhang X, Logemann E, Yu D, Wang J, Jirschtzka J *et al.* 2020. Direct pathogen-induced assembly of an NLR immune receptor complex to form a holoenzyme. *Science* 370: abe3069.

- Mahdi LK, Huang M, Zhang X, Nakano RT, Kopp LB, Saur IML, Jacob F, Kovacova V, Lapin D, Parker JE *et al.* 2020. Discovery of a family of mixed lineage kinase domain-like proteins in plants and their role in innate immune signaling. *Cell Host & Microbe* 28: 813–824.
- Manik MK, Shi Y, Li S, Zaydman MA, Damaraju N, Eastman S, Smith TG, Gu W, Masic V, Mosaibab T *et al.* 2022. Cyclic ADP ribose isomers: production, chemical structures, and immune signaling. *Science* 377: eadc8969.
- Martin R, Qi T, Zhang H, Liu F, King M, Toth C, Nogales E, Staskawicz BJ. 2020. Structure of the activated ROQ1 resistosome directly recognizing the pathogen effector XopQ. *Science* 370: eabd9993.
- Mindrebo JT, Nartey CM, Seto Y, Burkard MD, Noel JP. 2016. Unveiling the functional diversity of the alpha/beta hydrolase superfamily in the plant kingdom. *Current Opinion in Structural Biology* 41: 256–257.
- Mirdita M, Schütze K, Moriwaki Y, Heo L, Ovchinnikov S, Steinegger M. 2022. ColabFold: making protein folding accessible to all. *Nature Methods* 19: 679–682.
- Narusaka M, Shirasu K, Noutoshi Y, Kubo Y, Shiraishi T, Iwabuchi M, Narusaka Y. 2009. *RRS1* and *RPS4* provide a dual Resistance-gene system against fungal and bacterial pathogens. *The Plant Journal* 60: 218–226.
- Ngou BPM, Ahn HK, Ding P, Jones JDG. 2021. Mutual potentiation of plant immunity by cell-surface and intracellular receptors. *Nature* 592: 110–115.
- Ofir G, Herbst E, Baroz M, Cohen D, Millman A, Doron S, Tal N, Malheiro DBA, Malitsky S, Amitai G *et al.* 2021. Antiviral activity of bacterial TIR domains via immune signalling molecules. *Nature* 600: 116–120.
- Ordon J, Gantner J, Kemna J, Schwalgun L, Reschke M, Streubel J, Boch J, Stuttmann J. 2017. Generation of chromosomal deletions in dicotyledonous plants employing a user-friendly genome editing toolkit. *The Plant Journal* 89: 155–168.
- Ordon J, Martin P, Erickson JL, Ferik F, Balcke G, Bonas U, Stuttmann J. 2021. Disentangling cause and consequence: genetic dissection of the *DANGEROUS MIX2* risk locus, and activation of the DM2h NLR in autoimmunity. *The Plant Journal* 106: 1008–1023.
- Parker JE, Hessler G, Cui H. 2022. A new biochemistry connecting pathogen detection to induced defense in plants. *New Phytologist* 234: 819–826.
- Postma J, Liebrand TW, Bi G, Evrard A, Bye RR, Mbengue M, Kuhn H, Joosten MH, Robatzek S. 2016. *Avr4* promotes Cf-4 receptor-like protein association with the BAK1/SERK3 receptor-like kinase to initiate receptor endocytosis and plant immunity. *New Phytologist* 210: 627–642.
- Prautsch J, Erickson JL, Özyürek S, Gormanns R, Franke L, Parker JE, Stuttmann J, Schattat MH. 2021. XopQ induced stromule formation in *Nicotiana benthamiana* is causally linked to ETI signaling and depends on ADR1 and NRG1. *bioRxiv*. doi: 10.1101/2021.12.06.471425.
- Pruitt RN, Locci F, Wanke F, Zhang L, Saile SC, Joe A, Karelina D, Hua C, Frohlich K, Wan WL *et al.* 2021. The EDS1-PAD4-ADR1 node mediates Arabidopsis pattern-triggered immunity. *Nature* 598: 495–499.
- Qi T, Seong K, Thomazella DPT, Kim JR, Pham J, Seo E, Cho MJ, Schultink A, Staskawicz BJ. 2018. NRG1 functions downstream of EDS1 to regulate TIR-NLR-mediated plant immunity in *Nicotiana benthamiana*. *Proceedings of the National Academy of Sciences, USA* 115: E10979–E10987.
- Rauwerdink A, Kazlauskas RJ. 2015. How the same core catalytic machinery catalyzes 17 different reactions: the serine-histidine-aspartate catalytic triad of  $\alpha/\beta$ -hydrolase fold enzymes. *ACS Catalysis* 5: 6153–6176.
- Saijo Y, Loo EP, Yasuda S. 2018. Pattern recognition receptors and signaling in plant-microbe interactions. *The Plant Journal* 93: 592–613.
- Saile SC, Ackermann FM, Sunil S, Keicher J, Bayless A, Bonardi V, Wan L, Doumane M, Stobbe E, Jaillais Y *et al.* 2021. Arabidopsis ADR1 helper NLR immune receptors localize and function at the plasma membrane in a phospholipid dependent manner. *New Phytologist* 232: 2440–2456.
- Saile SC, Jacob P, Castel B, Jubic LM, Salas-Gonzales I, Backer M, Jones JDG, Dangl JL, El Kasmi F. 2020. Two unequally redundant “helper” immune receptor families mediate *Arabidopsis thaliana* intracellular “sensor” immune receptor functions. *PLoS Biology* 18: e3000783.
- Saucet SB, Ma Y, Sarris PF, Furzer OJ, Sohn KH, Jones JD. 2015. Two linked pairs of Arabidopsis TNL resistance genes independently confer recognition of bacterial effector AvrRps4. *Nature Communications* 6: 6338.
- Schultink A, Qi T, Lee A, Steinbrenner AD, Staskawicz B. 2017. Roq1 mediates recognition of the Xanthomonas and Pseudomonas effector proteins XopQ and HopQ1. *The Plant Journal* 92: 787–795.
- Seto Y, Yasui R, Kameoka H, Tamiru M, Cao M, Terauchi R, Sakurada A, Hirano R, Kisugi T, Hanada A *et al.* 2019. Strigolactone perception and deactivation by a hydrolase receptor DWARF14. *Nature Communications* 10: 191.
- Shimada A, Ueguchi-Tanaka M, Nakatsu T, Nakajima M, Naoe Y, Ohmiya H, Kato H, Matsuoka M. 2008. Structural basis for gibberellin recognition by its receptor GID1. *Nature* 456: 520–523.
- Shimada TL, Shimada T, Hara-Nishimura I. 2010. A rapid and non-destructive screenable marker, FAST, for identifying transformed seeds of *Arabidopsis thaliana*. *The Plant Journal* 61: 519–528.
- Sinapidou E, Williams K, Nott L, Bahkt S, Tor M, Crute I, Bittner-Eddy P, Beynon J. 2004. Two TIR:NB:LRR genes are required to specify resistance to *Peronospora parasitica* isolate Cala2 in Arabidopsis. *The Plant Journal* 38: 898–909.
- Stuttmann J, Barthel K, Martin P, Ordon J, Erickson JL, Herr R, Ferik F, Kretschmer C, Berner T, Keilwagen J *et al.* 2021. Highly efficient multiplex editing: one-shot generation of 8x *Nicotiana benthamiana* and 12x Arabidopsis mutants. *The Plant Journal* 106: 8–22.
- Stuttmann J, Hubberten HM, Rietz S, Kaur J, Muskett P, Guerois R, Bednarek P, Hoefgen R, Parker JE. 2011. Perturbation of Arabidopsis amino acid metabolism causes incompatibility with the adapted biotrophic pathogen *Hyaloperonospora arabidopsidis*. *Plant Cell* 23: 2788–2803.
- Stuttmann J, Peine N, Garcia AV, Wagner C, Choudhury SR, Wang Y, James GV, Griebel T, Alcazar R, Tsuda K *et al.* 2016. *Arabidopsis thaliana* DM2h (R8) within the Landsberg *RPPI-like* resistance locus underlies three different cases of EDS1-conditioned autoimmunity. *PLoS Genetics* 12: e1005990.
- Sun X, Lapin D, Feehan JM, Stolze SC, Kramer K, Dongus JA, Rzemieniewski J, Blanvillain-Baufumé S, Harzen A, Bautor J *et al.* 2021. Pathogen effector recognition-dependent association of NRG1 with EDS1 and SAG101 in TNL receptor immunity. *Nature Communications* 12: 3335.
- Takemoto D, Rafiqi M, Hurley U, Lawrence GJ, Bernoux M, Hardham AR, Ellis JG, Dodds PN, Jones DA. 2012. N-terminal motifs in some plant disease resistance proteins function in membrane attachment and contribute to disease resistance. *Molecular Plant-Microbe Interactions* 25: 379–392.
- Tao Y, Xie ZY, Chen WQ, Glazebrook J, Chang HS, Han B, Zhu T, Zou GZ, Katagiri F. 2003. Quantitative nature of Arabidopsis responses during compatible and incompatible interactions with the bacterial pathogen *Pseudomonas syringae*. *Plant Cell* 15: 317–330.
- Thieme F, Koebnik R, Bekel T, Berger C, Boch J, Buttner D, Caldana C, Gaigalat L, Goesmann A, Kay S *et al.* 2005. Insights into genome plasticity and pathogenicity of the plant pathogenic bacterium *Xanthomonas campestris* pv. *vesicatoria* revealed by the complete genome sequence. *Journal of Bacteriology* 187: 7254–7266.
- Thomma BPHJ, Nürnberger T, Joosten MHAJ. 2011. Of PAMPs and effectors: the blurred PTI-ETI dichotomy. *Plant Cell* 23: 4–15.
- Tian H, Wu Z, Chen S, Ao K, Huang W, Yaghmaiean H, Sun T, Xu F, Zhang Y, Wang S *et al.* 2021. Activation of TIR signalling boosts pattern-triggered immunity. *Nature* 598: 500–503.
- Van de Weyer AL, Monteiro F, Furzer OJ, Nishimura MT, Cevik V, Witek K, Jones JDG, Dangl JL, Weigel D, Bemm F. 2019. A species-wide inventory of NLR genes and alleles in *Arabidopsis thaliana*. *Cell* 178: 1260–1272.
- Van der Hoorn RA, Laurent F, Roth R, De Wit PJ. 2000. Agroinfiltration is a versatile tool that facilitates comparative analyses of Avr9/Cf-9-induced and Avr4/Cf-4-induced necrosis. *Molecular Plant-Microbe Interactions* 13: 439–446.
- Voss M, Toelzer C, Bhandari DD, Parker JE, Niefind K. 2019. Arabidopsis immunity regulator EDS1 in a PAD4/SAG101-unbound form is a monomer with an inherently inactive conformation. *Journal of Structural Biology* 208: 107390.
- Wagner S, Stuttmann J, Rietz S, Guerois R, Brunstein E, Bautor J, Niefind K, Parker JE. 2013. Structural basis for signaling by exclusive EDS1 heteromeric complexes with SAG101 or PAD4 in plant innate immunity. *Cell Host & Microbe* 14: 619–630.
- Wan L, Essuman K, Anderson RG, Sasaki Y, Monteiro F, Chung EH, Nishimura EO, DiAntonio A, Milbrandt J, Dangl JL *et al.* 2019. TIR domains of plant immune receptors are NAD<sup>+</sup>-cleaving enzymes that promote cell death. *Science* 365: 799–803.

- Wang J, Hu M, Wang J, Qi J, Han Z, Wang G, Qi Y, Wang HW, Zhou JM, Chai J. 2019. Reconstitution and structure of a plant NLR resistosome conferring immunity. *Science* 364: aav5870.
- Wen W, Meinkoth JL, Tsien RY, Taylor SS. 1995. Identification of a signal for rapid export of proteins from the nucleus. *Cell* 82: 463–473.
- Wirthmueller L, Zhang Y, Jones JD, Parker JE. 2007. Nuclear accumulation of the Arabidopsis immune receptor RPS4 is necessary for triggering EDS1-dependent defense. *Current Biology* 17: 2023–2029.
- Wu C-H, Abd-El-Halim A, Bozkurt TO, Belhaj K, Terauchi R, Vossen JH, Kamoun S. 2017. NLR network mediates immunity to diverse plant pathogens. *Proceedings of the National Academy of Sciences, USA* 114: 8113–8118.
- Wu Z, Li M, Dong OX, Xia S, Liang W, Bao Y, Wasteneys G, Li X. 2018. Differential regulation of TNL-mediated immune signaling by redundant helper CNLs. *New Phytologist* 222: 938–953.
- Wu Z, Tian L, Liu X, Zhang Y, Li X. 2021. TIR signal promotes interactions between lipase-like proteins and ADR1-L1 receptor and ADR1-L1 oligomerization. *Plant Physiology* 187: 681–686.
- Xiao S, Calis O, Patrick E, Zhang G, Charoenwattana P, Muskett P, Parker JE, Turner JG. 2005. The atypical resistance gene, *RPW8*, recruits components of basal defence for powdery mildew resistance in Arabidopsis. *The Plant Journal* 42: 95–110.
- Yu D, Song W, Tan EYJ, Liu L, Cao Y, Jirschitzka J, Li E, Logemann E, Xu C, Huang S *et al.* 2022. TIR domains of plant immune receptors are 2',3'-cAMP/cGMP synthetases mediating cell death. *Cell* 185: 2370–2386.
- Yuan M, Jiang Z, Bi G, Nomura K, Liu M, Wang Y, Cai B, Zhou JM, He SY, Xin XF. 2021. Pattern-recognition receptors are required for NLR-mediated plant immunity. *Nature* 592: 105–109.
- Zipfel C. 2014. Plant pattern-recognition receptors. *Trends in Immunology* 35: 345–351.

## Supporting Information

Additional Supporting Information may be found online in the Supporting Information section at the end of the article.

**Fig. S1** Generation of an *Nicotiana benthamiana bak1/serk3* mutant line by genome editing.

**Fig. S2** *Nicotiana benthamiana bak1* mutant plants are not impaired in cell death responses induced by intracellular pathways.

**Fig. S3** Cf-9/Avr9-induced cell death in *EDS1* family and *RNL* mutant *Nicotiana benthamiana* lines.

**Fig. S4** ROS burst assays with different flg22 concentrations in *Nicotiana benthamiana*.

**Fig. S5** Structural models (ALPHAFOLD2) of EDS1 complexes.

**Fig. S6** Stability of *S*EDS1 catalytic triad variants, and complex formation with *SSAG101b*.

**Fig. S7** Cell death assays with *S*EDS1 variants and overexpression of *SAG101b* from *Nicotiana benthamiana* or tomato.

**Fig. S8** Immunodetection of *S*EDS1-*SPAD4*, and variants thereof, in transgenic Arabidopsis.

**Fig. S9** Immunodetection of *S*EDS1 lid deletion variants and exchanges in proximity of the catalytic triad.

**Fig. S10** Immune-competence of mislocalized *SSAG101b* and protein accumulation of *S*EDS1 and *SSAG101b* mislocalization variants.

**Methods S1** Protein structural modeling using AF2.

**Table S1** Gene models for *Nicotiana benthamiana BAK1/SERK3*-like genes.

**Table S2** Plasmids used in this study.

**Table S3** Oligonucleotides used in this study.

Please note: Wiley Blackwell are not responsible for the content or functionality of any Supporting Information supplied by the authors. Any queries (other than missing material) should be directed to the *New Phytologist* Central Office.